Master thesis

New reference genes in *Trichoderma reesei*

Submitted for the purpose of obtaining the academic degree

Master of Science (MSc)

Under the supervision of

Associate Prof. Dipl.-Ing.in Dr.in techn. Astrid Mach-Aigner

(E166 - Institute of Chemical, Environmental and Bioscience Engineering, Research Unit Biochemical Technology)

and

Univ.Ass.in MSc Caroline Danner

(E166 - Institute of Chemical, Environmental and Bioscience Engineering, Research Unit Biochemical Technology)

Submitted to Vienna University of Technology (TU Wien)

Faculty of Technical Chemistry

by

JURIY KARPENKO

[redacted]

Table of content

Acknowledgements

I would like to express my gratitude to Prof. Astrid Mach-Aigner for giving me the opportunity to conduct my master's thesis in her research group. I am also very thankful to all group members for their help and support throughout my time here. A special thanks goes to my direct supervisor, Caroline Danner, for striking the perfect balance between guidance, assistance, and providing me with challenging tasks. I truly enjoyed my time in the research group, and the experience passed by far too quickly.

I would also like to extend my thanks to my family, friends, and colleagues for their unwavering support and motivation. In particular, I am grateful for the wonderful friends I made during my master's studies, who turned even the most stressful times into enjoyable moments. Without you, this journey would have been much more difficult, and the past two and a half years would not have been as memorable and fulfilling.

Abbreviations

cDNA	Complementary DNA
Ct-value	Cycle threshold value
CV	Coefficient of variation
dNTP	Deoxyribose nucleoside triphosphate
DTT	Dithiothreitol
GAPDH	Glyceraldehyde 3-phosphate dehydrogenase
M	Molar
MA	Mandels-Andreotti
PCR	Polymerase chain reaction
qPCR	Quantitative polymerase chain reaction
RT-PCR	Reverse transcription polymerase chain reaction
RT-qPCR	Reverse transcriptase quantitative polymerase chain reaction

Abstract

Trichoderma reesei is a highly significant producer of various enzymes used in industry and agriculture. Due to its relatively high secretion efficiency, it holds potential for a wide range of applications. However, the complexity of its gene expression mechanisms and the unpredictable behavior of newly developed genetically modified strains have made it a subject of extensive research. A particularly important method for gene expression analysis is the RT-qPCR, which requires stably expressed reference genes to ensure reliable results. The absence of properly evaluated reference genes, assessed using modern techniques, poses a significant challenge in qPCR-based research on *Trichoderma reesei*. In this study, potential new reference genes for gene expression analysis via RT-qPCR were evaluated against the currently used reference genes, *act1* and *sar1*. Candidate genes were identified *in silico* by analyzing publicly available RNA-Seq datasets. Five potential reference genes with promising expression stability were validated by RT-qPCR analysis of biological samples collected under a wide range of experimental conditions. Both *in silico* and RT-qPCR analysis ranked the novel gene, *bzip*, which appears to play a role in histone methylation, as the most stable in terms of expression. Additionally, all five novel genes exhibited higher expression stability compared to *act1* and *sar1*. As a result of these findings, we propose using the gene pair *bzip*/*traff* instead of *act1*/*sar1* for RT-qPCR analysis in *Trichoderma reesei*.

1 Introduction

1.1 Trichoderma

The genus *Trichoderma* is a well-studied group of filamentous fungi of the phylum Ascomycota with currently more than 300 species being identified (1). The classification and taxonomy of filamentous fungi and *Trichoderma* specifically have been very challenging since some of them can be found in their asexual (anamorph) and sexual varieties (teleomorphs) with distinct morphologies (2) (Figure 1). There are multiple historical miss-attributions of teleomorph forms of *Trichoderma* to the genus *Hypocrea* that presently are only of a historical nature and not used anymore (3). With the rise of bioinformatics and genome sequencing techniques, more and more species are being reassigned correctly to the genus *Trichoderma* (1).

Figure 1: Example of very different morphologies of anamorph (asexual, filamentous) form of Trichoderma reesei (left) and its teleomorph analog that used to be referred to as Hypocrea jecorina (right)(4)

Trichoderma can be characterized as a genus of opportunistic, avirulent plant symbionts (5). Additionally, many members of the genus are known for their mycoparasitic behavior (6), and have huge potential to be used as biocontrol agents (7). They can serve as an alternative to conventional pest control, which is nowadays still dominated by chemicals with adverse additional effects on the environment and soil. Two important mechanisms that can be beneficial for agriculture are the antibiosis of possible agricultural pests and nutrient competitiveness of *Trichoderma* with other fungi, bacteria, or nematodes (8). Several *Trichoderma* species are additionally also showing positive effects on plant growth through symbiosis (9). Figure 2 provides an overview of the main plant beneficial mechanisms of *Trichoderma* species.

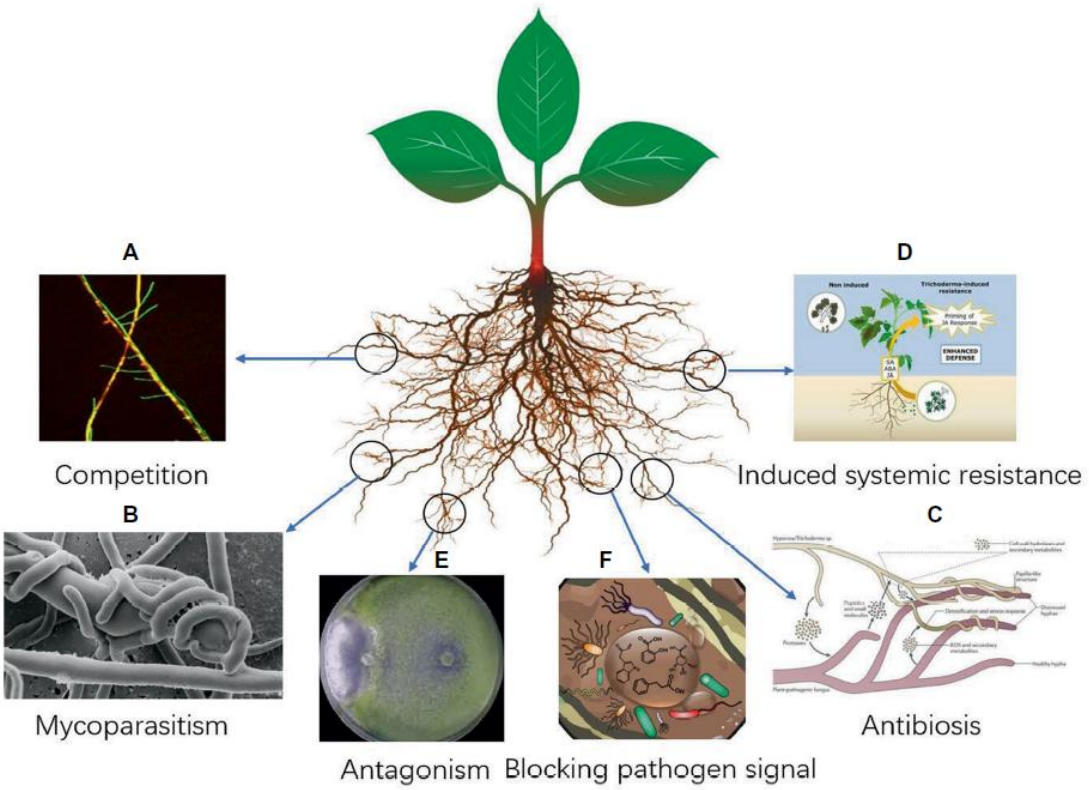

Figure 2: Overview of the plant-beneficial processes that Trichoderma is involved in (7)

The list of plant diseases and agricultural pests that *Trichoderma* is able to antagonize is long, but some prominent ones are presented in this paragraph (8). *T. harzianum* is a very versatile *Trichoderma* species with a wide range of fungal targets that may cause harm to plants, such as *Rhizoctonia solani* (10) and several *Fusarium* (11,12) species, among others. *T. asperellum, T. virens,* and *T. viride* are three other examples of organisms that can be used as a biocontrol against plant pathogens like *Pythium ultimum* (13), *Sclerotium rolfsii* (14) and *Botrytis cinerea* (15) amongst others. Most of these pathogens are responsible for plant rot, mold, and other general plant diseases, causing tremendous damage to agriculture.

1.1.1 *Trichoderma reesei*

The most investigated species of the genus *Trichoderma* is *Trichoderma reesei* (*T. reesei*). The fungus was first isolated during World War II on the Solomon Islands by the US Army. The stationed soldiers back then encountered the problem of their tents being degraded by fungi which led to the collection of multiple strains in that area for further investigation. One of the isolated strains was falsely identified as *Trichoderma virens* and named QM6a, as an abbreviation for the quartermaster who was assigned for this process (16–18). Years later, the strain was investigated by E. Reese and M. Mandels for its ability of cellulose degradation and, therefore, potential in biofuel production (18,19). They could show that the strain QM6a can be taxonomically distinguished from *T. virens* and after a temporal synonymizing with *Trichoderma longibrachiatum* in the 1980s (20), the strain QM6a could be identified and classified as its own taxon *T. reesei*. Furthermore, in the 1990s a connection between *T. reesei* and its teleomorph form *Hypocrea jecorina* could be proven (21). Since then, the name *H. jecorina* was used preferably for a while, until in 2013 it was decided to use *Trichoderma* as the only correct name for all holomorph species of both genera (3).

In the meantime, while the strain was still not correctly classified, research on QM6a was initiated which led to mutant strains that are still used in industry today. The first attempts resulted in the strain QM9414 that was received by mutations via two-step irradiation by a linear accelerator (22,23). A different attempt to screen for hyperproducing and enhanced *T. reesei* strains was conducted at Rutgers University, New Jersey. The strain QM6a was radiated by UV light and screened for strains not affected by catabolite repression, resulting in strain M7. In the next step that strain was genetically modified by contact with N-nitroguanidine, which resulted in the strain NG17 characterized by increased enzyme secretion and activity. Finally, this strain was again altered by another round of UV light and screened for high cellulase activity and resistance to 2-deoxyglucose, resulting in the strain Rut-C30 (24,25).

Rut-C30 shows a productivity of around 20 mg secreted protein per mL under controlled conditions which is roughly 15-20 times more than the wildtype strain QM6a (26). Additionally, Rut-C30 is unlike its parent strains, catabolite derepressed, and shows similar cellulase activities as in cellulose as in 5 % glycerin or 5 % glucose (24–26).

The strain Rut-C30 has become a major producing strain in the industry, is a target in research and is also used as a reference (27–29). Further optimization and screening of Rut-C30 are still leading to the isolation of new promising hyperproducing strains (30,31).

1.1.2 *T. reesei* as an industrial enzyme producer

Due to its saprophytic lifecycle, *T. reesei* is natively a producer of a wide palette of cellulases and other plant-biomass degrading enzymes. A big portion of the total secreted enzymes is three groups of cellulases: endoglucanases, exoglucanases, and β-glucosidases (32).

The application of cellulases produced by *T. reesei* in detergents has been practiced since the 1970s. With the addition of endoglucanases, loose cotton fibers in denim fabrics are degraded to some extent, leading to the loss of indigo dye enclosed in the fabrics. Subsequently, the denim textile gets a stone-washed appearance, without the actual use of pumice stones. This enzymatic method is often referred to as "bio-stoning" and its main benefit is a gentler treatment of the material and also energy efficiency. Another desired effect of using cellulases in detergents is generally a softening effect on the textiles after washing (33,34). *T. reesei* cellulases are also used in the food and feed industry. For example, in malting of grain (35) and other processes in beer brewing. Here a reduced content of glucans in the barley can be beneficial for the brewing process (36). Another significant application of enzymes produced by *Trichoderma* is the paper and pulp industry. Cellulases and hemicellulases produced by *T. reesei* and other filamentous fungi hold great potential as aids in paper production processes (37,38). Due to the versatility of the enzyme mix secreted by *Trichoderma* and the complexity of their interactions, specific enzymes offer distinct advantages and limitations. For instance, the use of purified cellobiohydrolase I (CBH1) has been shown to significantly reduce energy consumption, whereas similar benefits were not observed when the raw material was treated with the entire cellulase mix (39).

T. reesei also produces and secretes other types of plant biomass-degrading enzymes like hemicellulases (40) and lytic monooxygenases (41). Hemicellulases, such as xylanase from *T. reesei*, are particularly useful for lignin extraction and bio-bleaching of kraft pulp (42). Digestive enzyme supplements, often derived from filamentous fungi such as *Trichoderma* species, serve multiple purposes, including the elimination of anti-nutritional factors, the degradation of specific components to enhance nutritional value, and acting as supplemental enzymes to aid in the animals' digestive systems (35). Specifically, enzymes like glucanases, cellulases, and xylanases from *Trichoderma* are utilized in livestock feed to improve fiber digestibility (43).

All these enzymes act synergistically to degrade macromolecules like cellulose and hemicellulose that are present in plant biomass. A schematic overview of those reactions is presented in Figure 3. Possessing a broad repertoire of plant biomass-degrading enzymes coupled with a high productivity of up to 100 g/L of total secreted enzymes in hyperproducing strains (44), *T. reesei* has already been an industrial working horse for many decades.

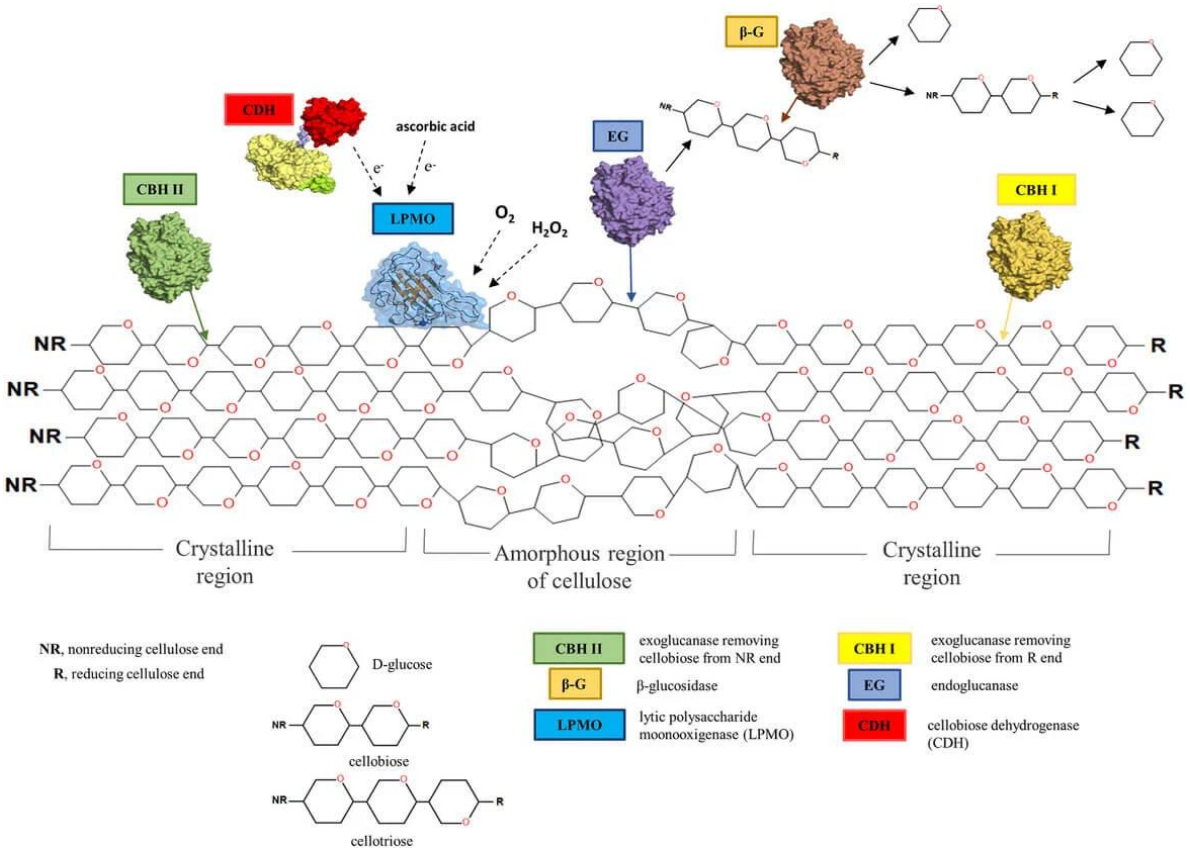

Figure 3: Enzymatic degradation of cellulose chain via synergistic interaction of cellulases (endoglucanase, exoglucanase, and β-glucosidase) and LPMO enzymes (45)

1.1.3 Heterologous protein production

Due to its high enzyme productivity and efficient secretion capabilities, *T. reesei* holds significant potential as a producer of non-native enzymes introduced into the organism via transformation.

The primary focus of heterologous protein expression in *T. reesei* has been to further enhance its plant biomass-degrading abilities. For instance, laccase from *Trametes* sp. (46) and xylanase B from *Dictyoglomus thermophilum* (47) have been introduced to improve xylan degradability.

Other examples of heterologous gene expression in *T. reesei* include lipase B (CalB) from *Candida antarctica* (48), chicken egg protein ovalbumin (49), and bovine chymosin, which was among the first non-native proteins expressed in *T. reesei* (50).

The most prominent transformation methods for *T. reesei* include polyethylene-glycol mediated transformation of protoplasts (51), transformation via *Agrobacterium tumefaciens* system (52), and electroporation (53). Additionally, CRISPR/Cas9 (54), a gene-editing system that has emerged over the past decade, is also used for gene deletions and insertions in *T. reesei* (55).

1.1.4 Potential in biofuel production

Due to its potent mix of plant biomass-degrading enzymes, *T. reesei* is especially interesting for bioethanol and biofuel production. The fungus not only produces these enzymes but also possesses the basic biochemical pathway to ferment biomass sugars into ethanol, albeit at low rates and yields (56).

Recent research has been focusing on enhancing *T. reesei*'s ethanol production capabilities through genetic engineering. By expressing genes from *Saccharomyces cerevisiae* coding for ethanol production enzymes, researchers have, for instance, achieved significant increases in ethanol yield and decreases in the formation of unwanted byproducts (56).

While *T. reesei* remains the industry standard, alternatives such as *Penicillium* and *Acremonium* species are being explored for their competitive enzyme production and hydrolytic performance (57). Ongoing research aims to optimize *T. reesei* strains and explore new isolates, to further improve bioethanol production efficiency (58,59).

1.2 Gene expression analysis

Gene expression analysis refers to the study of transcription levels of specific genes or entire genomes, as well as the evaluation of differences between samples. This type of analysis is crucial in biochemical sciences, particularly for investigating metabolomic mechanisms. The methods employed in gene expression analysis are designed to detect and quantify RNA, either directly or indirectly, in biological samples (60,61).

Early methods for RNA detection included Northern blot and RNase protection assay (62,63). However, these techniques have largely been superseded due to their time-consuming nature and the use of problematic chemicals.

DNA hybridization arrays, also known as DNA microarrays, offer an alternative approach that allows for the relative quantification of whole transcriptomes (60,64). This method is based on fluorescent-dye-stained RNA binding specifically to single-stranded DNA immobilized on commercially produced arrays. The primary advantage of this technique is its ability to evaluate thousands of genes simultaneously. However, it is limited by the number of available organisms that can be investigated and the relatively high cost (60).

In the 1990s, quantitative PCR (covered in detail in 1.3.2) emerged as a more cost-efficient method with the ability to analyze also novel organisms. This technique has largely replaced earlier methods due to its significant advantages (60).

With notable progress in nucleotide sequencing over recent decades and the rise of bioinformatics methods, a completely different approach to gene expression analysis became

available: RNA sequencing (RNA-Seq). RNA-Seq has revolutionized gene expression analysis by leveraging second-generation sequencing technologies and relatively low costs. This approach enables comprehensive exploration of transcription levels across entire transcriptomes. In addition to quantifying gene expression, RNA-Seq allows researchers to identify stably expressed genes, which are crucial for normalization in qPCR experiments (65,66).

Modern bioinformatical tools play a pivotal role in RNA-Seq analysis. These tools allow for the acquisition, processing, and extraction of gene counts from RNA-Seq files, followed by statistical analysis to identify significant patterns and differences. Commonly used bioinformatics pipelines include steps such as quality control, alignment of sequencing reads to a reference genome, transcript quantification, and differential expression analysis. Additionally, advanced algorithms can be applied to assess alternative splicing, detect novel transcripts, and integrate data into broader biological contexts (67).

The integration of bioinformatics into gene expression analysis has not only improved the accuracy and scope of research but also facilitated the study of previously inaccessible organisms and systems. As these technologies continue to evolve, the field of gene expression analysis is expected to provide even greater insights into the complex regulatory mechanisms underlying biological processes.

1.3 Polymerase chain reaction

1.3.1 Conventional PCR

Since the first description of the polymerase chain reaction (PCR) in the 1980s (68), it has become one of the most commonly used techniques in biomedical and biochemical research. Because of its simplicity and also the possibility to detect even trace amounts of DNA in samples, PCR has become an indispensable technique in research, clinical diagnostics and forensics.

In general, the method is used to amplify a specific DNA section in a thermal cycler. PCR usually requires forward and reverse primers that are specific to the DNA section of interest, a dNTP mix, a heat-resistant DNA polymerase, and a suitable buffer. The main stages in the thermal cycle consist of denaturation, annealing, and extension steps, where after each cycle the number of copies of the DNA template is theoretically doubled (69). Figure 4 depicts an overview of the main steps of a PCR cycle.

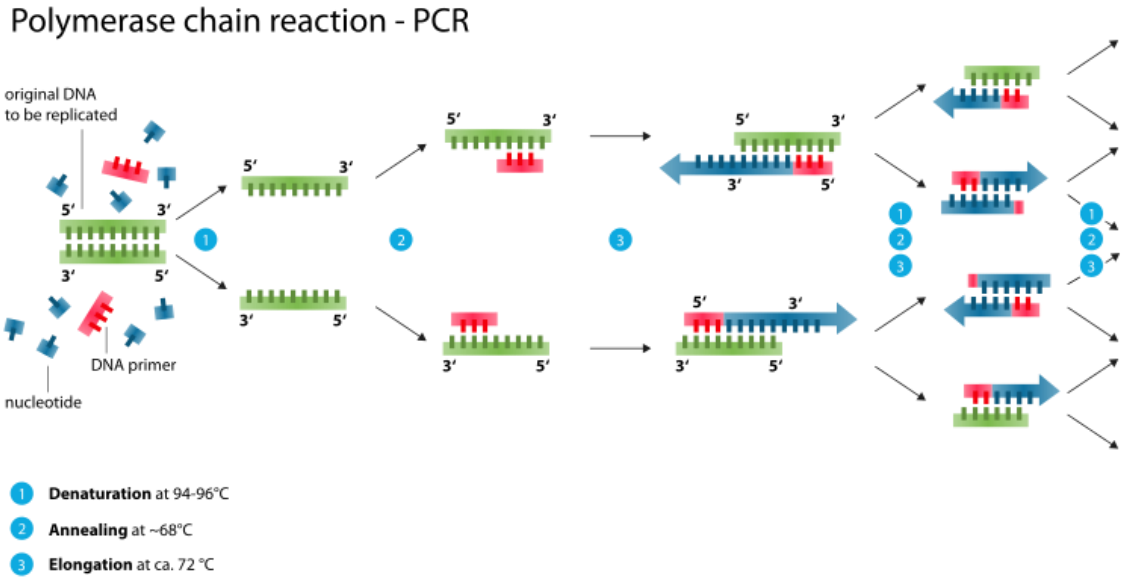

Figure 4: Schematic drawing of the PCR cycle (70)

The denaturation step requires relatively high temperatures of 94-96 °C to loosen the bonds between both strands of the DNA. In the second step, which is conducted at around 68 °C, both forward and reverse primers anneal to the template DNA. The exact temperature in this step can vary depending on the length and composition of the primers. In the third step of elongation which is performed at around 72 °C, the DNA polymerase assembles the complementary DNA strand. After the elongation, the cycle is repeated 30-40 times depending on the PCR application (69).

When the principle of PCR was invented, the DNA polymerase had to be added freshly after each denaturation step, since it was deactivated at high temperatures. This process was significantly simplified by the discovery of the first thermally stable polymerase from the extreme thermophile *Thermus aquaticus* (71). The DNA polymerase (*Taq*) isolated from this microorganism is nowadays still the most commonly used polymerase in PCR. The *Taq*-polymerase has exonuclease activity in 5' to 3' direction and an activity optimum at 72 °C, which explains the temperature used in the elongation step. At optimum temperature, *Taq* polymerizes around 150 base pairs per second (72).

Over time, more thermally stable DNA polymerases were discovered which can be used optionally instead of *Taq*, depending on their advantages. One of them is the DNA polymerase *Pfu*, that was isolated from *Pyrococcus furiosus* and is special because of its 3' to 5' exonuclease function. This additional proofreading function makes this polymerase less error-prone compared to *Taq*, but the amplification is slower as a downside (73).

Yet another example of a different DNA polymerase that can be used in PCR is Vent, isolated from the archaeal thermophile *Thermococcus litoralis*. This polymerase is characterized by its

extreme thermostability and also possesses a 3' to 5' exonuclease activity, making it like *Pfu,* another high-fidelity DNA polymerase (74). Because of its longevity in extreme conditions, it can be used for amplification of especially long DNA fragments (75).

Another very important aspect of the PCR process is the concentration of Mg^{2+} ions. Magnesium ions are usually brought into the reaction mix in the form of $MgCl_2$ salt and fulfill several functions. On one hand, Mg^{2+} is a cofactor for the DNA polymerase and is required for the polymerization reaction. Furthermore, Mg^{2+} ions act as stabilizers of the single-stranded DNA molecules and contribute to an easier attachment of the primers. The concentration of Mg^{2+} is one of the main adjusting parameters in PCR, because higher concentrations lead to a higher yield, but are making the process more error-prone. A much too high Mg^{2+} concentration even causes stabilization of the double-stranded DNA and non-functionality of the whole process (76).

To be able to detect specific RNA sequences in samples, the so-called reverse transcription polymerase chain reaction (RT-PCR) was developed. Here, a reverse transcriptase that originates from viruses is introduced along with either specific primers or oligo-T primers to attach to the poly-adenylated tails of all mRNA molecules (77). In this first step, complementary DNA (cDNA) is synthesized, which can then be analyzed like in the conventional PCR.

1.3.2 Quantitative PCR

The common PCR can, however, not be used for precise quantitative analysis of DNA in the samples. Only clues of abundance differences across samples can be gained by loading stained PCR products on agarose gels and comparing the intensity levels. To analyze relative or even absolute quantity of template DNA or RNA in biochemical samples, quantitative polymerase chain reaction (qPCR) or real-time PCR was developed (78).

Unlike conventional PCR, qPCR monitors the amplification of DNA throughout the entire process. The main mechanism in this method is the measurement of fluorescent light that increases after each amplification cycle. This increase in fluorescence can be used to determine either the relative abundance of a specific DNA sequence by comparing it to a reference gene (sometimes also referred to as internal control gene or housekeeping gene), or the absolute quantity, if using a reference of exactly known number of template copies (79).

Figure 5 illustrates a usual recording of fluorescence during a qPCR run. Fluorescence measurements of the samples are plotted against the cycle number, resulting in a characteristic amplification curve. At the beginning of the reaction, fluorescence cannot be distinguished from background noise, but at a specific point, known as the threshold, the signal becomes sufficiently intense and begins to increase exponentially. This phase continues until the reaction

reaches the saturation phase, where at least one of the components is depleted, leading to the termination of the chain reaction and a plateau in fluorescence (80).

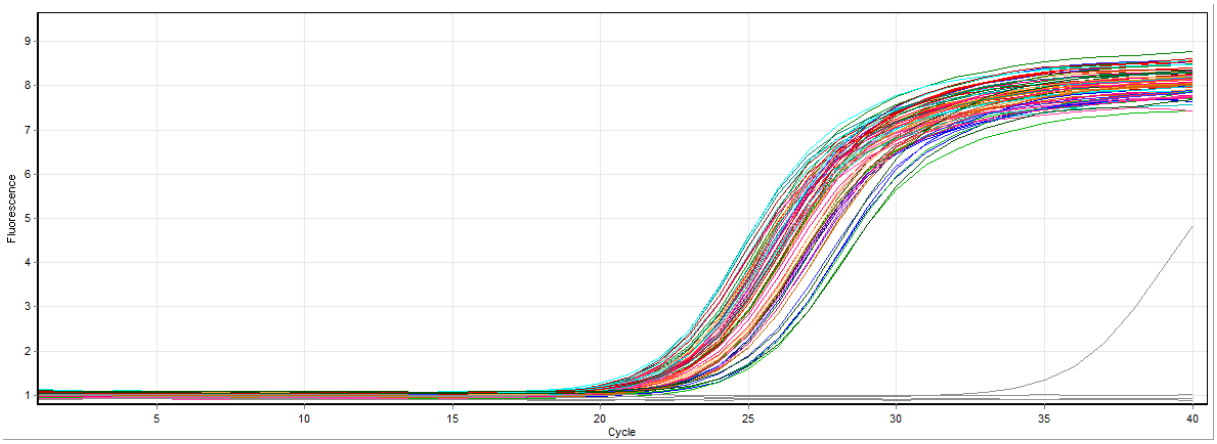

Figure 5: Fluorescence progression in a usual qPCR run. Colored curves represent samples with present specific cDNA that is amplified over time resulting in an amplification curve with an exponential part and saturation phase. The grey curves represent blind samples containing water instead of biological samples

A crucial parameter for qPCR calculations is the threshold cycle (Ct) value, which represents the cycle number at which the signal enters the exponential phase. Additionally, the slope of the amplification curve during this phase provides a measure of the practical amplification efficiency, an important factor for assessing the reliability of the qPCR results (78).

To quantify nucleotides via qPCR, at least one reference gene is required. Reference genes (covered in more detail in section 0) are considered to be stably expressed across all experimental conditions. By assuming a constant relative concentration of mRNA for these genes in all samples, the abundance of mRNA for genes of interest can be reliably compared across different samples (81).

The two main methods to implement fluorescence in qPCR are non-specific dyes that attach to any kind of double-stranded DNA and the use of specific reporter probes (82). The non-specific method (for example, SYBR® Green) uses fluorescent dyes that intercalate into any double-stranded DNA, thereby gaining their fluorescent properties. The fluorescence is measured at the end of each extension step, before the denaturation step in each cycle (78).

For the specific detection method, a more sophisticated approach is used (for example TaqMan®). The fluorescent agent is added along with a quencher on the ends of specific probes. As long as the quencher is in the proximity of the fluorescent part of the probe, all fluorescent properties are suppressed. Only after attachment to the template and subsequent degradation of the probe by the 5'-3' exonuclease activity of *Taq* polymerase does the marker gain its fluorescent properties. This way, fluorescence increases after each extension step (83). Figure 6 depicts a graphical comparison of both methods with the examples of SYBR® Green and TaqMan®.

While the non-specific method is the cheaper option, there is the possibility of background noise, since the non-specific dye can also bind to non-target DNA sequences such as primer dimers. The main disadvantage of the TaqMan system is the additional time and financial cost to design specific probes, but is rewarded by more precise and specific results (78).

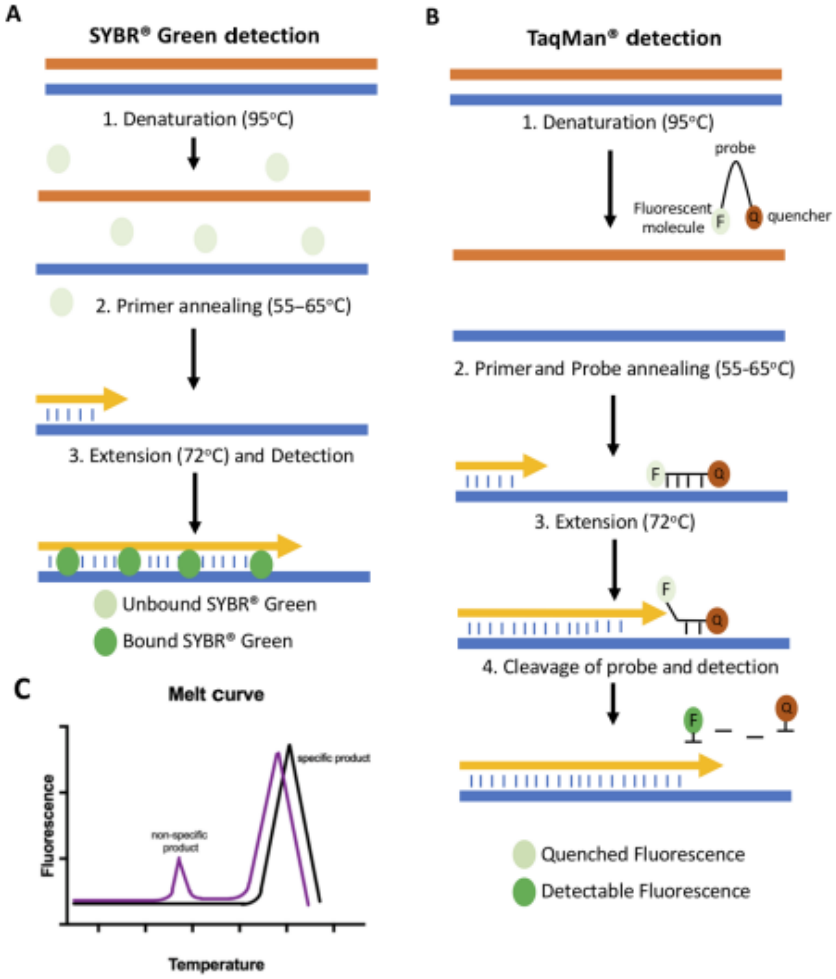

Figure 6: Comparison of non-specific and specific probe detection in qPCR (84)

Reverse transcription-quantitative polymerase chain reaction (RT-qPCR) is a powerful technique that combines reverse transcription (RT) of RNA into complementary DNA (cDNA) with quantitative PCR (qPCR) to allow detection and quantification of specific RNA targets. This method has become the most important technique for gene expression analysis due to its high sensitivity, specificity, and wide dynamic range. RT-qPCR allows researchers to measure the abundance of gene-specific transcripts and monitor changes in gene expression under various experimental conditions (82).

1.3.3 Reference genes in qPCR

As mentioned above, the choice of one or multiple appropriate reference genes is crucial for the representativeness and credibility of RT-qPCR results. When RT-qPCR was developed in the 1990s, methods for evaluating expression stability were limited. At that time, reference genes were selected based on the assumption that their functions remained active under all experimental conditions (81). The term *housekeeping gene* was commonly used in this context, as these genes typically encode products involved in fundamental cellular functions. Common examples include actin, GAPDH, ubiquitin, and ribosomal RNAs (85).

However, with continuous advancements in gene expression analysis and the development of improved methods for evaluating expression stability, these "classical" housekeeping genes have been shown to be not always suitable as reference genes (86). Even though they are involved in essential cellular processes, their expression can still be influenced by specific experimental conditions (87).

Significant progress in selecting appropriate reference genes for qPCR began with the 1st International qPCR Symposium in Germany (March 2004) and was further reinforced by the publication of the MIQE Guidelines (Minimum Information for Publication of Quantitative Real-Time PCR Experiments) in 2009 (81). These guidelines emphasize the key requirements for reliable reference genes: most importantly, stable expression across a wide range of experimental conditions, a relatively high expression level, and expression levels comparable to those of the genes of interest. Additionally, the use of multiple reference genes is recommended (81,86,88).

Since the establishment of these guidelines and, in particular, with advancements in computational performance, various methods for evaluating gene expression stability have been developed. Notable examples include the M-value method (89), the comparative ΔCt-method (90), BestKeeper (91), NormFinder (92) and GeNorm (93). Tools such as RefFinder (94), which integrate multiple methods and calculate the most stable genes based on Ct values alone, have further simplified the evaluation process.

Another increasingly important approach in reference gene evaluation involves bioinformatics. By analyzing RNA-Seq data, researchers can now identify previously unrecognized genes across the entire transcriptome that have the potential to serve as reference genes for qPCR (95).

In recent decades, numerous studies on filamentous fungi and yeasts have demonstrated that some classical housekeeping genes do not meet the stability requirements needed for reference genes, and better alternatives have been identified. For instance, Tao et al. (96) found that previously used reference genes were unsuitable for *Volvariella volvacea* and identified novel candidates with superior performance. Similar studies on *Amylostereum areolatum* (97) and

Komagataella phaffii (*Pichia pastoris*) (98,99) also led to the discovery of new reference genes for qPCR. In 2010, a study on *T. reesei* identified *sar1* as the most stable gene among those investigated. However, this study considered only a limited number of candidate genes that had performed well in other filamentous fungi (100). With the advent of modern bioinformatics methods, the pool of potential reference genes has expanded, offering better-suited candidates for future research.

2 Aims of the thesis

Since the exact mechanisms and regulation of enzyme production in *T. reesei* are not yet fully understood or well-documented, further research is needed. RT-qPCR is currently a widely used method for investigating gene expression, including in *T. reesei*. However, under extreme conditions and in newly developed industrial strains, the commonly used reference genes *act1* and *sar1* may not always be the most suitable choices.

The primary objectives of this thesis are to characterize the stability of *act1* and *sar1* expression and to verify whether they are suitable reference genes for qPCR. Simultaneously, the study aims to identify alternative genes that remain stable under various conditions. These objectives arise from the lack of gene expression stability analyses using bioinformatics methods in recent studies on *T. reesei*.

To achieve these goals, a bioinformatics approach will be employed to identify suitable candidate genes from the entire *T. reesei* transcriptome. Once identified, these candidate genes will be validated through qPCR analysis using samples from a broad range of conditions. Ideally, the newly identified candidates will outperform the established reference genes *act1* and *sar1*, making them promising alternatives for future *T. reesei* research.

Another key question is whether the bioinformatics predictions align with the RT-qPCR results. If the two approaches yield consistent findings, it would significantly simplify future reference gene selection for other organisms as well.

3 Materials and methods

3.1 Bioinformatics

Several publicly available RNA-seq datasets of the *T. reesei* strains QM6a and Rut-C30 were found on the SRA page of NCBI and the compressed files were retrieved from the EBI FTP database (101). An overview of the experimental conditions and technical specifics of the RNA-Seq data can be found in the annex (sections 9.1 and 9.2).

The raw reads were processed on the Unix-based Debian 12 operating system using HISAT2 (v2.2.1) (102), SAMtools (v1.16.1) (103,104) and featureCounts (v2.0.3) (105,106) to obtain raw counts for the RNA-seq data. This process required respective genomes and annotations. Exemplary scripts for these steps are provided in the annex (section 9.3).

The raw counts were normalized using the package DESeq2 (v1.14.0) (107) in RStudio (v2024.04.2 Build 764.) and subsequently exported as Excel files. Exemplary scripts for this process are included in the annex (section 9.4).

Since the genome annotations for QM6a (GenBank GCA_000167675.2) and Rut-C30 (GenBank GCA_000513815.1) differed, a list of orthologous genes was generated in Debian using gffread (v0.12.7) (108) and BLAST (v2.15.0) (109), both installed via the Bioconda package manager (v3.3.1). This step was necessary to enable direct comparison of gene expression between the two strains.

To compare gene stability in both strains, the coefficient of variation (CV) was calculated for each gene present in both datasets. Additionally, raw RNA counts from a third *T. reesei* strain, GEN-3A, were analyzed in the same manner. GEN-3A is an industrial strain developed by Genencor® (CA, USA) and derived from the *T. reesei* strain RL-P37.

In total, 31 raw gene count datasets obtained from the cultivation of GEN-3A under induced and non-induced conditions at multiple time points were processed in Excel to calculate CVs for all charted genes. However, many genes in GEN-3A were not properly annotated, limiting the ability to assess their expression stability. Nevertheless, using the available information, potential candidate genes were identified or excluded if their CVs were too high in GEN-3A.

The selection of candidate genes was further refined by filtering out lowly expressed genes, as they are not suitable for the use as control genes in qPCR. This was performed manually in Excel by calculating the average gene count in each condition, and using this value as reference. The idea was, that for a gene to be used as a reference gene, it should at least have an above average expression level.

3.2 Cultivations

For the experiments, the *T. reesei* strains QM6a, Rut-C30, RL-P37, and GEN-3A were used. The strains were cultured in a Mandels-Andreotti minimal medium with a 1 % carbon source. Additionally, an industrial-inducing medium and two stress conditions were applied.

Figure 7: Cultivation in MA minimal medium of different T. reesei strains resulting in different coloring of the media

3.2.1 Minimal media

Glucose, lactose, xylan, glycerin, and cellulose were used as different carbon sources. The media were composed of a phosphate-citrate buffer, a mineral salt solution, a trace element solution, and a 1 % carbon source. Table 1 shows the composition of the three main components of the Mandels-Andreotti media. For the phosphate-citrate buffer, di-sodium hydrogen phosphate was dissolved in 500 mL of water, the pH was adjusted to 5 with citric acid, and the volume was brought up to 1 L.

Table 1: Composition of the main components of Mandels-Andreotti media

Phosphate-citrate buffer (1 L)	
$Na_2HPO_4 \cdot 2H_2O$	17,8 g
Mineral salt solution (1 L)	
$(NH_4)_2SO_4$	5,6 g
KH_2PO_4	8 g
$MgSO_4 \cdot 7H_2O$	1,2 g
$CaCl_2 \cdot 2H_2O$	1,6 g

Trace element solution (1 L)	
$FeSO_4 \cdot 7H_2O$	250 mg
$MnSO_4 \cdot H_2O$	85 mg
$ZnSO_4 \cdot 7H_2O$	70 mg
$CoCl_2 \cdot 6H_2O$	100 mg

Table 2 summarizes the composition of the media components. Sterile urea was added after autoclaving.

Table 2: Composition of the Mandels-Andreotti media

Component	in 1 L
Carbon source	10 g
Phosphate-citrate buffer	500 mL
Mineral salt solution	250 mL
Trace element solution	20 mL
Urea (5M)	1 mL
Peptone	1 g

3.2.2 Induction medium

An inducing medium provided by the company Genencor® was also used in the experiment. The exact composition of this medium is confident, but it contains sophorose to induce enzyme production in *T. reesei*.

3.2.3 Dithiothreitol

To simulate endoplasmic reticulum (ER) stress, dithiothreitol (DTT) was added after 72 hours of growth in 1 % lactose minimal medium, to a final concentration of 20 mM.

3.2.4 Osmotic stress

To simulate osmotic stress, a concentrated NaCl solution was added after 48 hours to a 1 % glucose minimal medium, bringing the final concentration to 1 M.

3.2.5 Incubation and harvesting

All cultivations were initiated at a spore OD_{600} of 0.05 in total volumes of either 50 mL or 200 mL, depending on the medium. The cultivations with minimal medium in non-stress conditions (glucose, glycerin, cellulose, xylan, and lactose) were conducted in 200 mL medium,

the three other conditions in 50 mL. The incubation temperature was 30 °C, with shaking at 180 rpm. The cultures were incubated in biological duplicates, and samples were taken at two time points, which varied depending on the strain and condition. An overview of all harvesting time points can be found in Table 3.

Table 3: Overview of the harvesting timepoints for each condition and strain. The numbers in each cell represent the two harvesting timepoints after inoculation or addition of DTT or NaCl

	QM6a	Rut-C30	RL-P37	GEN-3A
Glucose	36 h / 84 h	24 h / 84 h	24 h / 84 h	24 h / 84 h
Lactose	72 h / 96 h	48 h / 72 h	48 h / 72 h	48 h / 72 h
Xylan	24 h / 48 h	24 h / 48 h	24 h / 48 h	24 h / 48 h
Glycerin	24 h / 84 h	36 h / 84 h	24 h / 84 h	24 h / 84 h
Cellulose	48 h / 120 h	48 h / 120 h	48 h / 120 h	48 h / 120 h
Induction medium	48 h / 96 h	48 h / 96 h	48 h / 96 h	48 h / 96 h
Lactose-DTT	6 h / 48 h	6 h / 48 h	6 h / 48 h	6 h / 48 h
Glucose-NaCl	6 h / 24 h	6 h / 24 h	6 h / 24 h	6 h / 24 h

3.2.6 Sample collection

Sample volumes ranged from 2 to 12 mL, depending on the growth stage and mycelium density, and the samples were washed with ultra-pure sterile water after filtering on Mira Cloth. The mycelium was immediately placed into sterile cryo tubes and frozen in liquid nitrogen. The samples were stored in liquid nitrogen until RNA extraction.

3.3 RNA extraction

RNA extraction and purification were performed using the RNA extraction kit from Zymo Research (Zymo Research, CA, USA), following the manufacturer's protocol with minor modifications. Mycelium was disrupted using a FastPrep®-24 instrument (MP Biomedicals, USA). Approximately 100 mg of frozen mycelium were placed in screw-cap tubes containing 1 mL RNAzol, along with 0.37 g small glass beads (0.1 mm diameter), 0.25 g medium glass beads (1 mm diameter), and one large glass bead (5 mm diameter). The tubes were subjected to homogenization at intensity level 6 for 30 seconds. After homogenization, the tubes were incubated at room temperature for 5 minutes, then centrifuged at 12,000 × g for 5 minutes.

The aqueous phase (750 µL) was transferred to a fresh nuclease-free tube and mixed with an equal volume of 96 % ethanol. The mixture was applied to the RNA-binding columns in 500 µL aliquots, centrifuging each time at 16,000 × g for 30 seconds. The bound RNA was washed with 400 µL RNA Wash Buffer, followed by treatment with 5 µL DNase and 75 µL DNase buffer, incubating for 15 minutes at room temperature. The columns were further washed twice

with 400 µL RNA Pre-Wash Buffer and once with 700 µL RNA Wash Buffer, with 30-second centrifugation steps after each wash. A final 1-minute centrifugation step was performed to dry the columns completely.

RNA was eluted with 30 µL RNase-free water, and its concentration and purity were assessed using a NanoDrop One^{C} spectrophotometer (Thermo Fisher Scientific, USA).

3.4 cDNA synthesis

For cDNA synthesis, the LunaScript® RT SuperMix kit (New England Biolabs, USA) was used. RNA samples containing 500 ng total RNA were mixed with 2 µL RT SuperMix and adjusted to a final volume of 10 µL with RNase-free water. The cDNA synthesis was performed on a T100 Thermal Cycler (Bio-Rad Laboratories, CA, USA) following the program outlined in Table 4.

Table 4: cDNA synthesis program

25 °C	2 min
55 °C	10 min
95 °C	1 min
4 °C	hold infinitely

The resulting cDNA was diluted 1:50 in ultrapure water for use in qPCR and subsequent storage.

3.5 RT-qPCR

The Luna® Universal (RT)-qPCR kit (New England Biolabs, USA) was used for qPCR. The composition of the qPCR master mix is shown in Table 5. The primer pairs for each gene were designed in Unipro UGENE v50.0 with standard settings for qPCR (110). The sequences and properties of those primers can be found in the annex (Section 9.5).

Table 5: Composition of the master mix used for qPCR analysis

	Volume per sample
Luna® Universal qPCR mix	7.5 µL
Ultra-pure water	4.75 µL
Forward primer	0.375 µL
Reverse primer	0.375 µL

Each reaction consisted of 2 µL of diluted cDNA and 13 µL of master mix, and measurements were performed in technical duplicates.

The qPCR was conducted using a Rotor-Gene Q system (QIAGEN, Germany) equipped with version 2.3.1 software. Automatic sample mixing was performed by a QIAgility pipetting robot (QIAGEN, Germany). The qPCR program is detailed in Table 6.

Table 6: Program used for qPCR analysis

Process	Temperature	Duration
Initial denaturation	95 °C	1 min
40x Cycling of denaturation and elongation	95 °C 60 °C	15 sec 30 sec
Melting point analysis of the products	60-95 °C	1 °C per 5 sec

3.6 Expression stability analysis

For further analysis, Ct values from each RT-qPCR run were extracted using the Rotor-Gene Q software (version 2.3.1). Amplification efficiency was calculated for each run using the software's internal tools and did not fall below 1.74 in all runs.

The Ct values of technical duplicates were averaged for each condition and consolidated into a single Excel file. To evaluate the stability of all seven genes, RefFinder was utilized (94). In addition to generating an overall ranking that encompassed all 128 conditions, various subgroups of conditions were also analyzed. The function of GeNorm (93) to identify the most stable reference gene pair was also utilized. By grouping of the samples and their resulting Ct-values according strains, media or harvesting timepoints into distinct subgroups, potential differences in these conditions could be uncovered.

4 Results and Discussion

4.1 Evaluation of results from the bioinformatics analysis

The bioinformatic analysis yielded a list of potential new reference genes for *T. reseei*. Table 7 lists the five chosen candidates with very low CV values, which indicates a high gene expression stability and shows the potential of that gene to be used as a reference gene. Due to the annotation issues in the count data of the strain GEN-3A, not all genes could be accounted for in those datasets and do not have CV values in the table.

Table 7: Gene IDs and descriptions of five chosen candidate reference genes based on the CV values in the three T. reesei strains QM6a, Rut-C30 and GEN-3A and the established reference genes act1 and sar1

Gene ID	Description	CV in QM6a	CV in Rut-C30	CV in GEN-3A
TRIREDRAFT_50536	bZIP domain containing protein (*bzip*)	0,1450	0,1038	0,3081
TRIREDRAFT_49838	Trafficking protein particle complex subunit 1 (*traff*)	0,2169	0,0993	0,2545
TRIREDRAFT_29932	CUE domain containing protein (*cue*)	0,2743	0,1691	0,2059
TRIREDRAFT_61945	Ubiquitin-like 1-activating enzyme E1 B (*ubi1*)	0,1367	0,1340	-
TRIREDRAFT_5916	Histone acetyltransferase (*sas3*)	0,1787	0,1237	-
TRIREDRAFT_44504	Actin (*act1)*	0,3725	0,3534	0,4744
TRIREDRAFT_61470	Secretion associated Ras related GTPase (*sar1)*	0,9250	0,6846	-

In general, the five new candidate genes were selected based on the lowest coefficient of variation (CV) values across all three strains. In this regard, *bzip*, *traff*, and *cue* were the top-performing genes, as they also met the requirement of having above-average expression levels across all datasets. However, due to an annotation issue in the GEN-3A dataset, several genes could not be accounted for, meaning many potential candidate genes remained undetected. To address this, a separate summation of CV values was performed for the QM6a and Rut-C30 strains, specifically for genes that were not annotated in the GEN-3A dataset. As a result, the genes *ubi1* and *sas3*, which exhibited exceptionally low CV values in QM6a and Rut-C30, were identified and added to the list of candidate genes.

Since there was little or no information in literature on the genes *bzip*, *traff,* and *cue* on NCBI, further investigation was initiated to get an idea of those genes' functions in *T. reesei*.

For *bzip*, orthologs in multiple filamentous fungi of the subdivision *Pezizomycotina* (division of Ascomycota) could be found through the online resource eggNOG (111). Further search on the websites Uniprot.org and String-db.org led to the protein's predicted structure and clusters of other proteins that likely interact with this protein. By investigating multiple orthologs on String-db.org, connections to histone H4, several chromatin remodeling proteins, and arginine methyltransferase could be found. Furthermore, the ortholog in *Fusarium oxysporum f. sp. cubense*, had already a name that was assigned to it by Guo L. et al. in the course of genome sequencing and annotation of this organism (112) and the name "bZIP domain containing protein" was adopted for this work. Looking at the clues in regard of the functionality of the product of this gene, it is very likely a factor in the process of histone methylation.

Information about *traff* regarding its predicted function could be retrieved from NCBI. The gene product of *traff*, according to NCBI, contains the so-called Gryzun domain, which is likely responsible for protein trafficking through membranes (113).

Both *cue* and *ubi1* are involved in the ubiquitination process. The gene product of *cue* contains the so-called CUE domain, which is a conserved sequence found in Ascomycota and exhibits weak ubiquitin-binding properties. Proteins containing this domain are reported to be involved in intramolecular monoubiquitylation (114). The gene *ubi1* is relatively well documented and codes for a ubiquitin-activating enzyme (E1) - subunit UBA2 and is responsible for ubiquitination and subsequent protein processing (115).

The histone acetyltransferase (*sas3*) contains the conserved MYST domain and is involved in the activation of gene transcription (116).

All five chosen potential reference genes show in general significantly lower CV values than *act1* and *sar1*, which is demonstrated graphically in Figure 8.

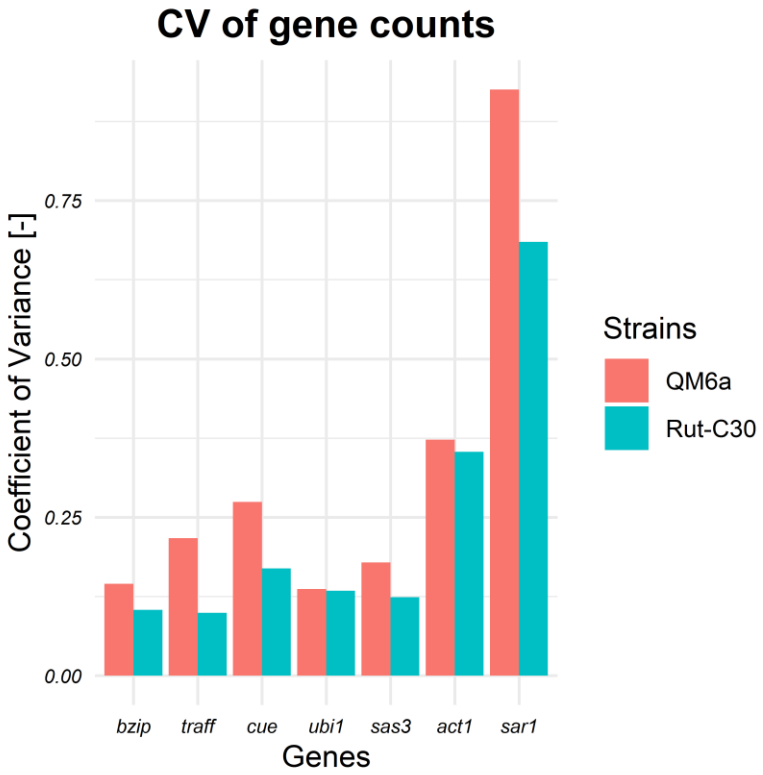

Figure 8: CV values of all seven candidate reference genes in the strains QM6a and Rut-C30

To rank all seven genes according expression stability CV values of the strains QM6a and Rut-C30 were summed and sorted from lowest to highest. Table 8 shows the sum and ranking of the genes in the strains QM6a and Rut-C30.

Table 8: Sum of CV values of both QM6a and Rut-C30 strains, resulting in a ranking of stability

Rank	Gene	Summed CV
1	*bzip*	0,2488
2	*ubi1*	0,2707
3	*sas3*	0,3024
4	*traff*	0,3162
5	*cue*	0,4434
6	*act1*	0,7259
7	*sar1*	1,6096

4.2 RT-qPCR and RefFinder

4.2.1 Analysis of the gene stability ranking in all tested cultivation conditions

Figure 9 shows the overall ranking of the five novel candidates as well the established genes *act1* and *sar1* across all 128 samples. The tool RefFinder identified *bzip* as the most stable and *act1* as the least stable gene.

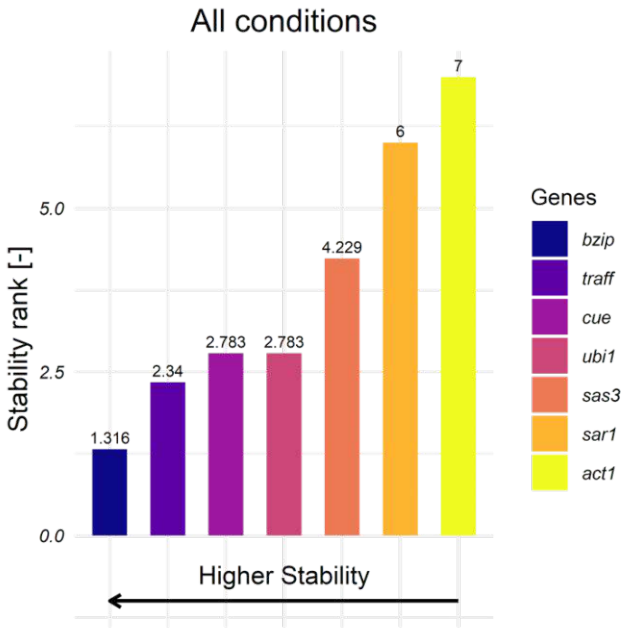

Figure 9: Expression stability ranking of the seven investigated reference genes throughout all conditions (94)

Additionally, GeNorm suggests the genes *bzip* and *traff* to be used as a pair of reference genes which is visualized in Figure 10.

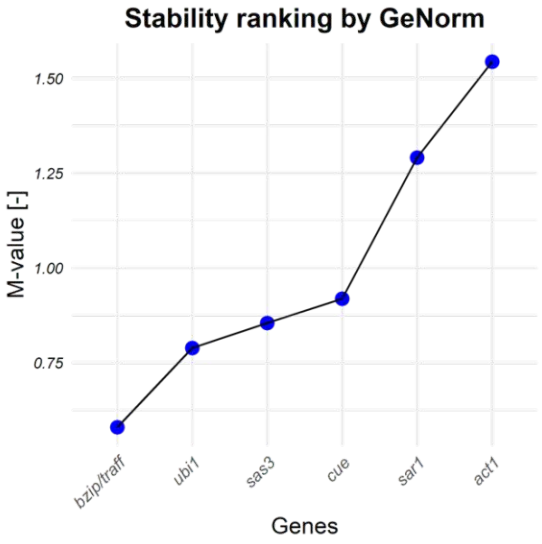

Figure 10: Expression stability ranking of the seven investigated reference genes throughout all conditions conducted only by GeNorm. A lower M-value represents a higher expression stability (93,94)

Since the expression stability analysis via RT-qPCR and RefFinder included an additional strain and covered in general different cultivation conditions than those of the available RNA-Seq files, this resulting ranking should not be directly compared to the bioinformatics results. Nevertheless, obvious similarities, like *bzip* being the most stable and the pair *act1* / *sar1* the least stable genes, can be highlighted.

4.2.2 Gene stability ranking in specific cultivation conditions or strains

Figure 11 shows the gene expression stability ranking considering only the strains QM6a and Rut-C30, while Figure 12 depicts the ranking for the strains QM6a, Rut-C30 and GEN-3A. The main idea behind these subgroups, was to check if there is a better matching with the ranking of combined CV values (Table 8), since they include only the strains that were analyzed in the bioinformatics approach. However, no differences in the ranking (Figure 11) or only the swapping of *ubi1* and *cue* (Figure 12) could be seen. This shows that there are minor changes to the results from the bioinformatics part. Nevertheless, *bzip* is always identified as the most stably expressed gene, and *act1* and *sar1* rank in the last places. A possible reason for not completely matching results is that the conditions that were used in the bioinformatics part, differ from the ones used for RT-qPCR analysis. Although the conditions were very diverse, there is still the possibility of a certain bias in those data sets.

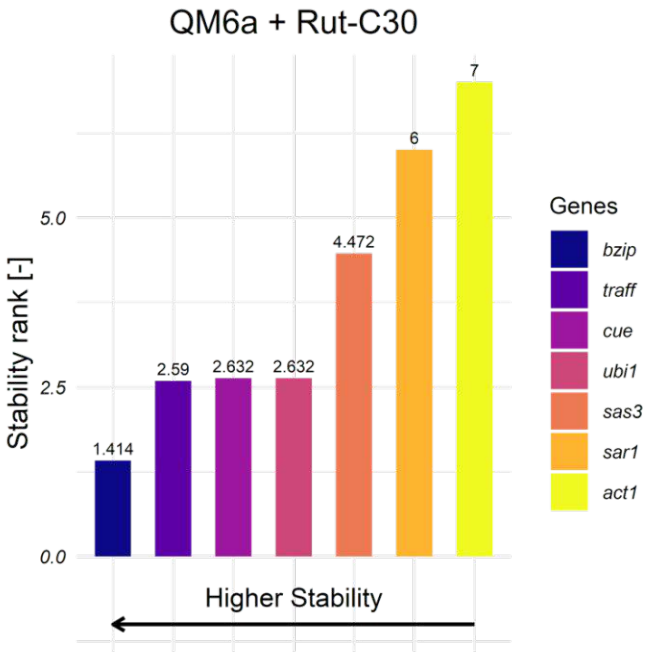

Figure 11: Expression stability ranking of the seven investigated reference genes in the strains QM6a and Rut-C30 (94)

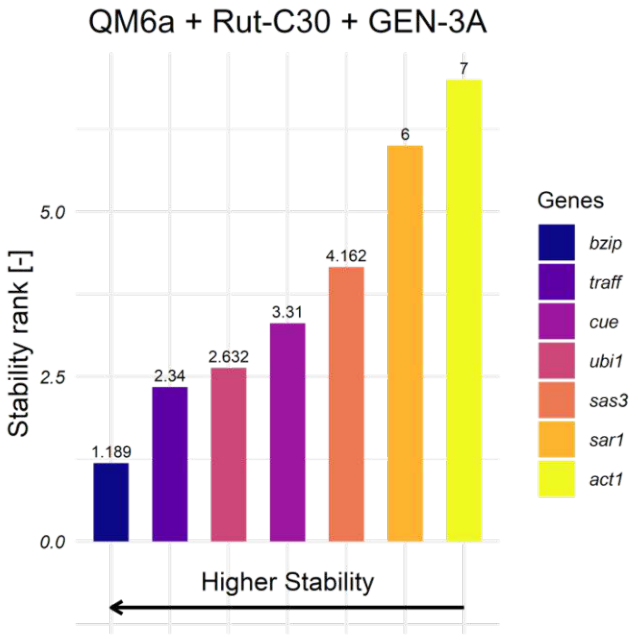

Figure 12: Expression stability ranking of the seven investigated reference genes in the strains QM6a, Rut-C30 and GEN-3A (94)

Figure 13 depicts gene expression stability ranking of all four strains under stress conditions (addition of DTT and NaCl) and non-stress conditions. Compared to the overall ranking, there are not many differences in these cases. The most striking one is the lower stability of *traff* in the stress conditions, nevertheless it is more stable than the genes *act1* and *sar1*. Looking at the subgroup of non-stress conditions, there are no differences to the overall expression stability ranking.

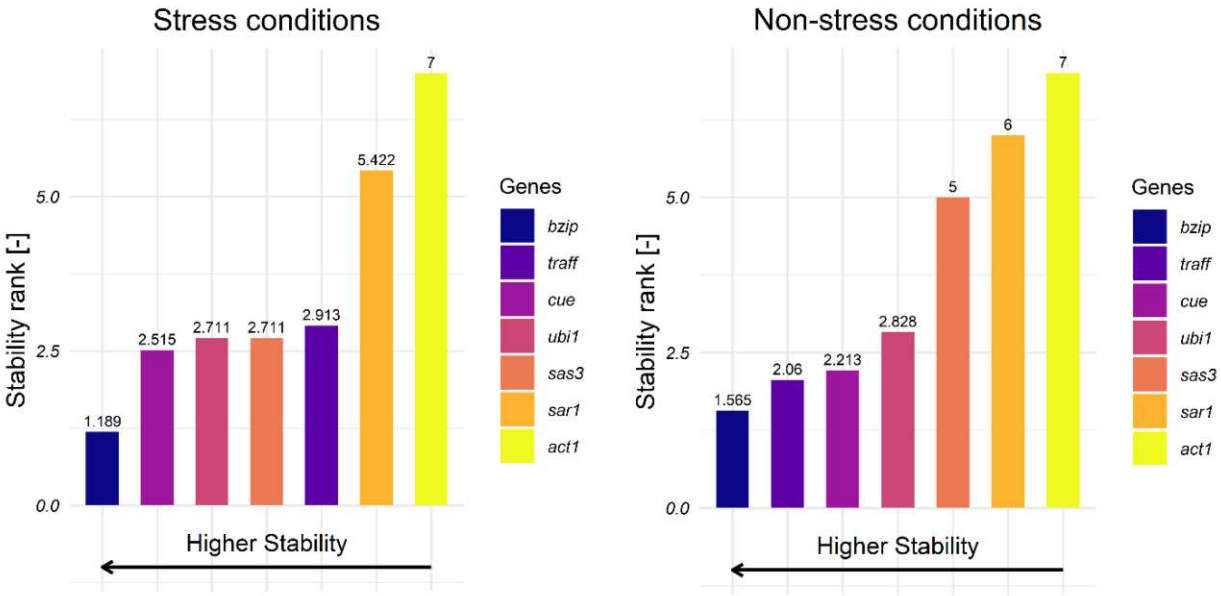

Figure 13: Expression stability ranking of the seven investigated reference genes of all four strains in stress conditions (left) and non-stress conditions (right) (94)

The next two subgroups focus of the type of carbon source (Figure 14). The subgroup of simple carbon sources only includes the conditions with glucose, lactose and glycerin, while complex carbon sources cover the conditions with xylan and cellulose. In the simple carbon source conditions, *act1* and *sar1* swap places in the ranking, but are still the two least stable genes. In the complex carbon source conditions *traff* is less stable than *cue*.

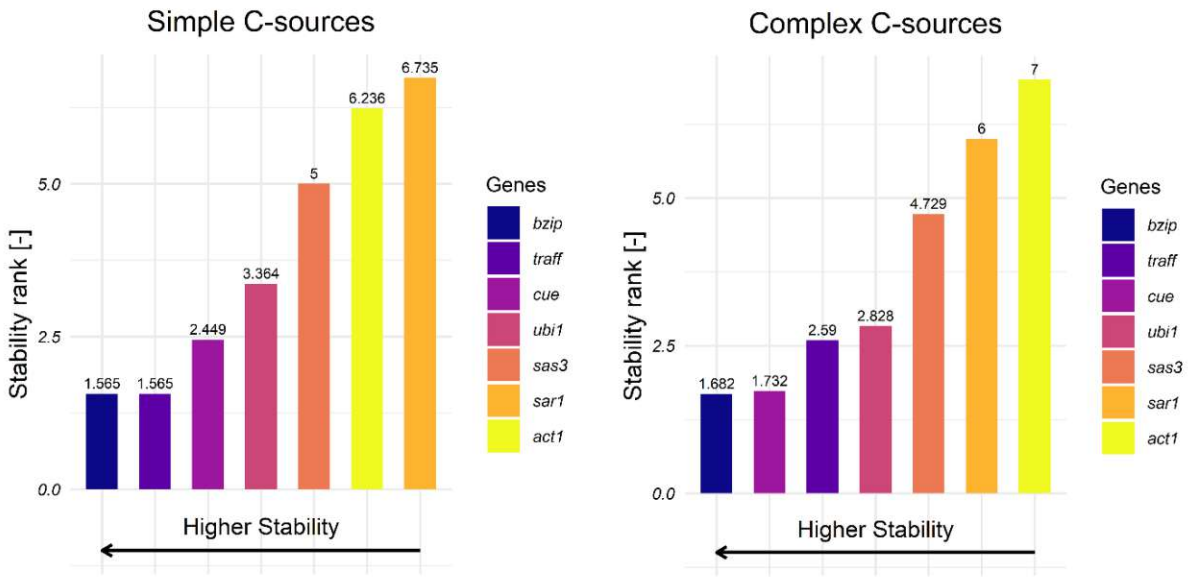

Figure 14: Expression stability ranking of the seven investigated reference genes of all four strains in media with simple carbon sources (left) and complex carbon sources (right) (94)

Figure 15 shows the gene expression stability in the four *T. reesei* strains if separated in subgroups. The ranking in the wildtype QM6a shows a lower stability of *traff* compared to the overall ranking, but does not have any other significant differences. In Rut-C30 and RL-P37, *sar1* moved up in the stability ranking, while *sas3* and *ubi1* respectively, are less stable. In RL-P37 *cue* was identified as the most stable gene, while *bzip* is ranked second. The gene stability ranking in GEN-3A shows no significant differences to the overall ranking, except *cue* being less stable.

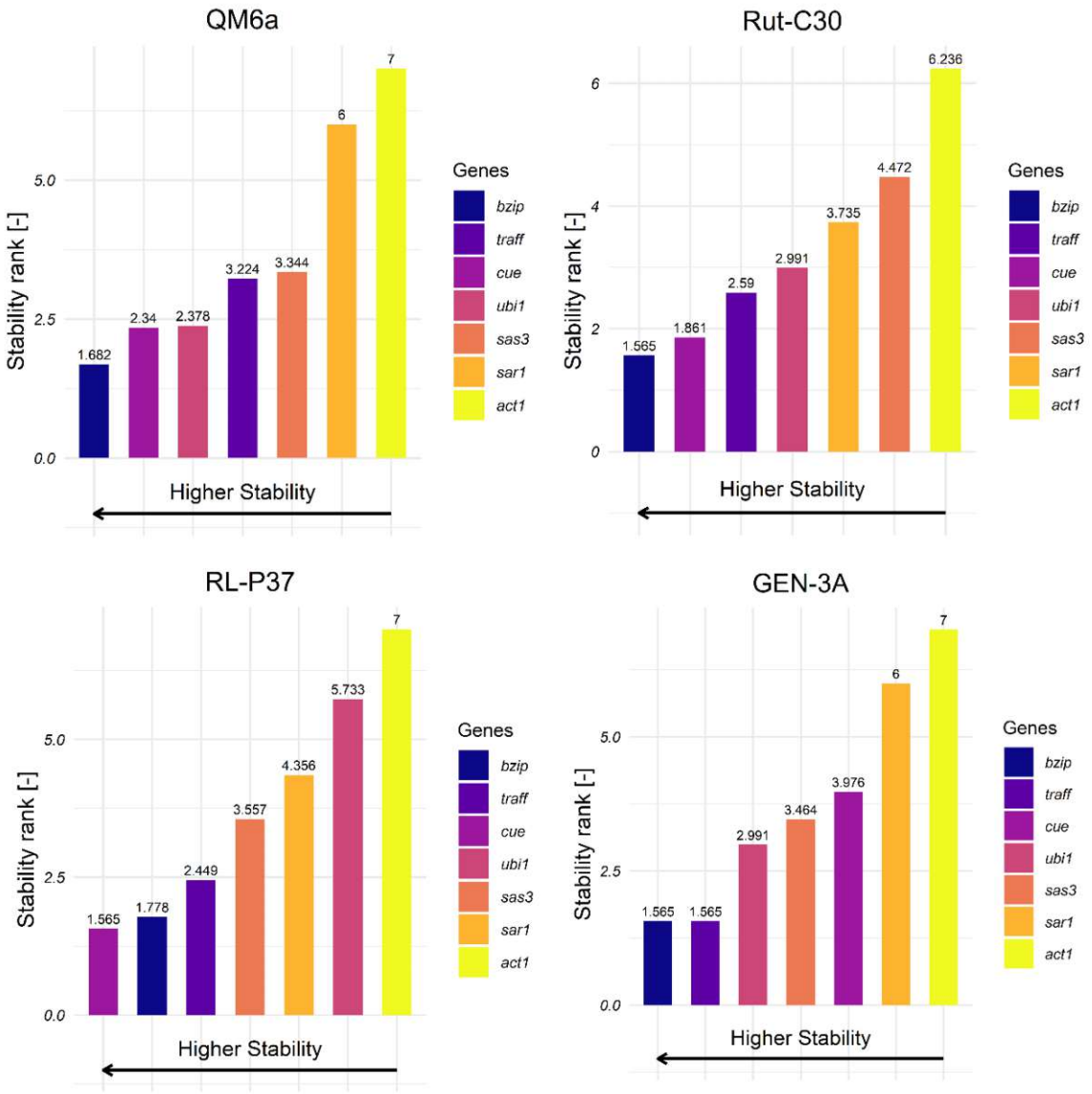

Figure 15: Expression stability ranking of the seven investigated reference genes of all four strains in separated subgroups (94)

Figure 16 depicts the gene expression stability ranking for early and late harvesting time points. The ranking in the early time points shows minimal changes compared to the overall ranking, whereas some notable changes are observed in the late time points. The genes *sas3* and *sar1* appear to be more stably expressed at later time points, although *sar1* still remains the second least stable gene in the ranking.

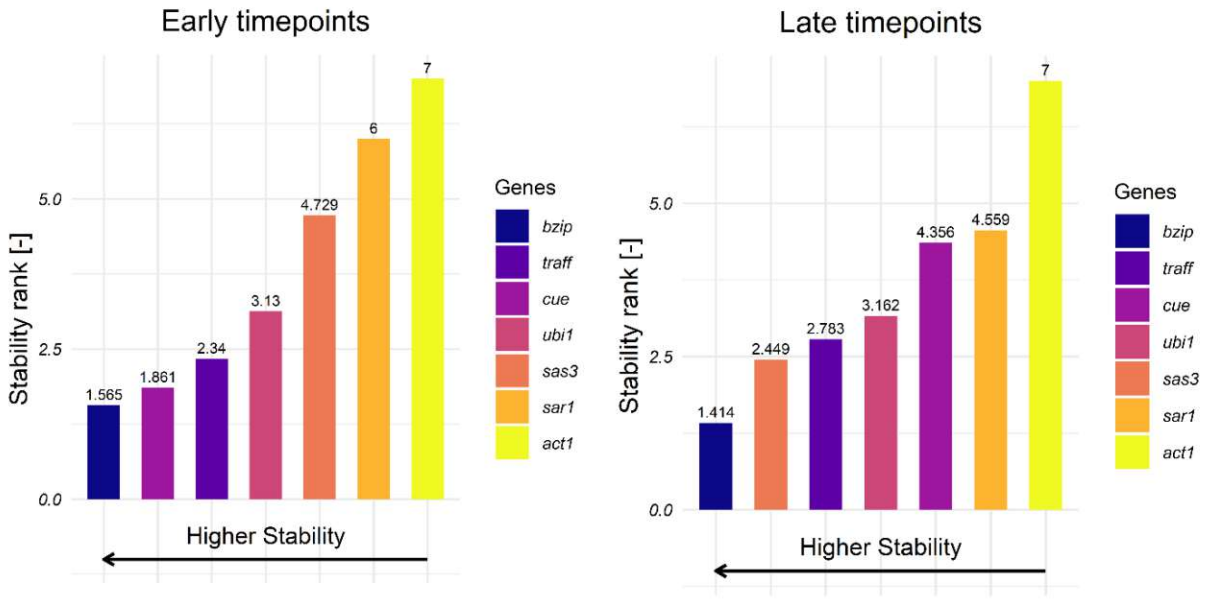

Figure 16: Expression stability ranking of the seven investigated reference genes of all four strains harvested at early (left) and late timepoints (right) (94)

5 Conclusion and outlook

The findings from the bioinformatics analysis led to the identification of five genes with high expression stability across three different strains of *T. reesei* under various cultivation conditions. These genes exhibited significantly more stable expression compared to the established reference genes *act1* and *sar1*. The results were validated through RT-qPCR, which revealed a highly similar ranking of these genes in terms of expression stability.

The bZIP-domain-containing protein (*bzip*) was identified as the most stable gene in both the bioinformatics analysis and RT-qPCR experiments. Its exceptional expression stability placed it first in the overall ranking, as well as in most subgroup rankings. Although the stability rankings of the other four genes did not perfectly align with the bioinformatics results, all four genes demonstrated greater stability than *act1* and *sar1* in nearly all subgroups and especially in the overall ranking.

These results are highly promising, and the next logical step would be to test these new reference genes in practical expression analyses using RT-qPCR, for example, by quantifying the expression of a known gene. It would be particularly interesting to compare differences in relative quantification when using *act1*/*sar1* versus *bzip*/*traff* as reference genes.

Another valuable experiment would involve investigating the orthologous genes in other organisms. Establishing the expression stability of these genes across different species would strengthen their potential as universal reference genes. Since all five newly identified genes have orthologs in at least the Pezizomycotina subgroup (filamentous fungi), their expression stability could be evaluated using the same approach applied in this study.

As a next step, the expression stability of these genes could be examined in species closely related to *T. reesei*. For organisms with publicly available RNA-Seq data, such as *Trichoderma virens*, *Trichoderma harzianum*, or *Trichoderma asperellum*, a preliminary assessment of expression stability could be performed relatively easily using bioinformatics methods. Additionally, it would be particularly interesting to evaluate the orthologs of these genes in industrially significant filamentous fungi, such as *Aspergillus niger* and *Penicillium chrysogenum*, as well as in agriculturally important pathogens, such as *Fusarium oxysporum*, which are active areas of contemporary research.

Since the bioinformatics results closely aligned with those from RT-qPCR, future research could potentially reduce or even eliminate the time- and resource-intensive cultivation steps, thereby streamlining the investigation of expression stability in other organisms.

6 List of figures

7 List of Tables

8 References

1. Tyśkiewicz R, Nowak A, Ozimek E, Jaroszuk-Ściseł J. *Trichoderma*: The Current Status of Its Application in Agriculture for the Biocontrol of Fungal Phytopathogens and Stimulation of Plant Growth. Int J Mol Sci. 2022 Feb 19;23(4).

2. Samuels GJ. *Trichoderma* : Systematics, the Sexual State, and Ecology. Phytopathology. 2006 Feb;96(2):195–206.

3. Hawksworth DL, Crous PW, Redhead SA, Reynolds DR, Samson RA, Seifert KA, et al. The Amsterdam Declaration on Fungal Nomenclature. IMA Fungus. 2011 Jun 7;2(1):105–11.

4. Ke Wenjun. Taiwan Encyclopedia of Life. Retrieved from https://taieol.tw/muse/digi_object/8446fb987b0d559164d64db3e37446f6#51365. 2016. *Hypocrea jecorina* photograph.

5. Harman GE, Howell CR, Viterbo A, Chet I, Lorito M. *Trichoderma* species — opportunistic, avirulent plant symbionts. Nat Rev Microbiol. 2004 Jan;2(1):43–56.

6. Harman GE. Overview of Mechanisms and Uses of *Trichoderma* spp. Phytopathology. 2006 Feb;96(2):190–4.

7. Yao X, Guo H, Zhang K, Zhao M, Ruan J, Chen J. *Trichoderma* and its role in biological control of plant fungal and nematode disease. Front Microbiol. 2023 May 3;14.

8. Verma M, Brar SK, Tyagi RD, Surampalli RY, Valéro JR. Antagonistic fungi, *Trichoderma* spp.: Panoply of biological control. Biochem Eng J. 2007 Oct;37(1):1–20.

9. Rebolledo-Prudencio OG, Dautt-Castro M, Estrada-Rivera M, González-López M del C, Jijón-Moreno S, Casas-Flores S. *Trichoderma* in the rhizosphere. In: New and Future Developments in Microbial Biotechnology and Bioengineering. Elsevier; 2020. p. 3–38.

10. Askew DJ, Laing MD. The in vitro screening of 118 *Trichoderma* isolates for antagonism to *Rhizoctonia solani* and an evaluation of different environmental sites of *Trichoderma* as sources of aggressive strains. Plant Soil. 1994 Feb;159(2):277–81.

11. Prasad RD, Rangeshwaran R, Hegde SV, Anuroop CP. Effect of soil and seed application of *Trichoderma harzianum* on pigeonpea wilt caused by *Fusarium udum* under field conditions. Crop Protection. 2002 May;21(4):293–7.

12. Calistru C, McLean M, Berjak P. In vitro studies on the potential for biological control of *Aspergillus flavus* and *Fusarium moniliforme* by *Trichoderma* species. Mycopathologia. 1997;137(2):115–24.

13. Roberts DP, Lohrke SM, Meyer SLF, Buyer JS, Bowers JH, Jacyn Baker C, et al. Biocontrol agents applied individually and in combination for suppression of soilborne diseases of cucumber. Crop Protection. 2005 Feb;24(2):141–55.

14. Mukherjee PK, Raghu K. *Trichoderma* sp. as a microbial suppressive agent of *Sclerotium rolfsii* on vegetables. World J Microbiol Biotechnol. 1997;13(5):497–9.

15. Cooney JM, Lauren DR. *Trichoderma* /pathogen interactions: measurement of antagonistic chemicals produced at the antagonist/pathogen interface using a tubular bioassay. Lett Appl Microbiol. 1998 Nov 9;27(5):283–6.

16. Mandels M, Reese ET. Induction of cellulase in *Trichoderma viride* as influenced by carbon sources and metals. J Bacteriol. 1957 Feb;73(2):269–78.

17. Siu RGH, Reese ET. Decomposition of cellulose by microorganisms. The Botanical Review. 1953 Jul;19(7):377–416.

18. Mandels M, Eveleigh DE. Reflections on the United States Military 1941-1987. Biotechnol Biofuels. 2009 Dec 1;2(1):20.

19. Simmons EG. Classification of some cellulase-producing *Trichoderma* species. In: Simmons EG (ed) Second International Mycological Congress. Tampa, Florida; 1977. p. 618.

20. Bissett J. A revision of the genus *Trichoderma* . I. Section *Longibrachiatum* sect. nov. Canadian Journal of Botany. 1984 May 1;62(5):924–31.

21. Kuhls K, Lieckfeldt E, Samuels GJ, Kovacs W, Meyer W, Petrini O, et al. Molecular evidence that the asexual industrial fungus *Trichoderma reesei* is a clonal derivative of the ascomycete *Hypocrea jecorina*. Proceedings of the National Academy of Sciences. 1996 Jul 23;93(15):7755–60.

22. Mandels M, Weber J, Parizek R. Enhanced Cellulase Production by a Mutant of *Trichoderma viride*. Appl Microbiol. 1971 Jan;21(1):152–4.

23. Montenecourt BS, Eveleigh DE. Preparation of mutants of *Trichoderma reesei* with enhanced cellulase production. Appl Environ Microbiol. 1977 Dec;34(6):777–82.

24. Montenecourt BS, Eveleigh DE. Selective Screening Methods for the Isolation of High Yielding Cellulase Mutants of *Trichoderma reesei*. In 1979. p. 289–301.

25. Peterson R, Nevalainen H. *Trichoderma reesei* Rut-C30 – thirty years of strain improvement. Microbiology (N Y). 2012 Jan 1;158(1):58–68.

26. Bisaria VS, Ghose TK. Biodegradation of cellulosic materials: Substrates, microorganisms, enzymes and products. Enzyme Microb Technol. 1981 Apr;3(2):90–104.

27. Fonseca LM, Parreiras LS, Murakami MT. Rational engineering of the *Trichoderma reesei* Rut-C30 strain into an industrially relevant platform for cellulase production. Biotechnol Biofuels. 2020 Dec 22;13(1):93.

28. Bailey MJ, Tähtiharju J. Efficient cellulase production by *Trichoderma reesei* in continuous cultivation on lactose medium with a computer-controlled feeding strategy. Appl Microbiol Biotechnol. 2003 Aug 1;62(2–3):156–62.

29. Singhania RR, Sukumaran RK, Pandey A. Improved Cellulase Production by *Trichoderma reesei* Rut-C30 under SSF Through Process Optimization. Appl Biochem Biotechnol. 2007 Sep 27;142(1):60–70.

30. Sheir-Neiss G, Montenecourt BS. Characterization of the secreted cellulases of *Trichoderma reesei* wild type and mutants during controlled fermentations. Appl Microbiol Biotechnol. 1984 Jul;20(1).

31. Luo Y, Valkonen M, Jackson RE, Palmer JM, Bhalla A, Nikolaev I, et al. Modification of transcriptional factor ACE3 enhances protein production in *Trichoderma reesei* in the absence of cellulase gene inducer. Biotechnol Biofuels. 2020 Dec 6;13(1):137.

32. de Paula RG, Antoniêto ACC, Ribeiro LFC, Carraro CB, Nogueira KMV, Lopes DCB, et al. New Genomic Approaches to Enhance Biomass Degradation by the Industrial Fungus *Trichoderma reesei*. Int J Genomics. 2018 Sep 24;2018:1–17.

33. Schuster A, Schmoll M. Biology and biotechnology of *Trichoderma*. Appl Microbiol Biotechnol. 2010 Jul 12;87(3):787–99.

34. Johanna Buchert, Tarja Oksanen, Jaakko Pere, Matti Siika-Aho, Anna Suurnäkki, Liisa Viikari. Applications of *Trichoderma reesei* enzymes in the pulp and paper industry. In: Gary E. Harman CPK, editor. Trichoderma and Gliocladium. LondonBristo: Taylor & Francis; 1998. p. 343–63.

35. Canales AM, Garza R, Sierra JA, Arnold R. The application of a β-glucanase with additional side activities in brewing. MBAA TQ. 1988;25:27–31.

36. Pajunen O. Optimal Use of β-Glucanases in Wort Production. EBC-Symposium on Wort Production, Monograph XI. 1986;137–48.

37. Bhat MK. Cellulases and related enzymes in biotechnology. Biotechnol Adv. 2000;18(5):355–83.

38. Suurnäkki A, Tenkanen M, Siika-aho M, Niku-Paavola ML, Viikari L, Buchert J. *Trichoderma reesei* cellulases and their core domains in the hydrolysis and modification of chemical pulp. Cellulose. 2000;7(2):189–209.

39. Pere J, Liukkonen S, Siika-aho M, Gullichsen J, Viikari L. Use of purified enzymes in mechanical pulping. Vol. 2, 1996 Tappi Pulping Conference. Atlanta: TAPPI Press; 1996. p. 693.

40. Juhász T, Szengyel Z, Réczey K, Siika-Aho M, Viikari L. Characterization of cellulases and hemicellulases produced by *Trichoderma reesei* on various carbon sources. Process Biochemistry. 2005 Nov;40(11):3519–25.

41. Adnan M, Ma X, Xie Y, Waheed A, Liu G. Heterologously Expressed Cellobiose Dehydrogenase Acts as Efficient Electron-Donor of Lytic Polysaccharide Monooxygenase for Cellulose Degradation in *Trichoderma reesei*. Int J Mol Sci. 2023 Dec 6;24(24):17202.

42. Suurnäkki A, Clark T, Allison R, Viikari L, Buchert J. Xylanase- and mannanase-aided ECF and TCF bleaching. Tappi J. 1996;79(7):111–7.

43. Iannaccone F, Alborino V, Dini I, Balestrieri A, Marra R, Davino R, et al. *In vitro* Application of Exogenous Fibrolytic Enzymes from *Trichoderma* spp. to Improve Feed Utilization by Ruminants. Agriculture. 2022 Apr 19;12(5):573.

44. Cherry JR, Fidantsef AL. Directed evolution of industrial enzymes: an update. Curr Opin Biotechnol. 2003 Aug;14(4):438–43.

45. Andlar M, Rezić T, Marđetko N, Kracher D, Ludwig R, Šantek B. Lignocellulose degradation: An overview of fungi and fungal enzymes involved in lignocellulose degradation. Eng Life Sci. 2018 Nov 27;18(11):768–78.

46. Zhang J, Hong Y, Li K, Sun Y, Yao C, Ling J, et al. Enhancing the production of a heterologous *Trametes* laccase (LacA) by replacement of the major cellulase CBH1 in *Trichoderma reesei*. J Ind Microbiol Biotechnol. 2023 Feb 17;50(1).

47. Te'o VS, Cziferszky AE, Bergquist PL, Nevalainen KM. Codon optimization of xylanase gene xynB from the thermophilic bacterium *Dictyoglomus thermophilum* for expression in the filamentous fungus *Trichoderma reesei*. FEMS Microbiol Lett. 2000 Sep 1;190(1):13–9.

48. Rantasalo A, Vitikainen M, Paasikallio T, Jäntti J, Landowski CP, Mojzita D. Novel genetic tools that enable highly pure protein production in *Trichoderma reesei*. Sci Rep. 2019 Mar 22;9(1):5032.

49. Järviö N, Parviainen T, Maljanen NL, Kobayashi Y, Kujanpää L, Ercili-Cura D, et al. Ovalbumin production using *Trichoderma reesei* culture and low-carbon energy could mitigate the environmental impacts of chicken-egg-derived ovalbumin. Nat Food. 2021 Dec 16;2(12):1005–13.

50. Harkki A, Uusitalo J, Bailey M, Penttilä M, Knowles JKC. A Novel Fungal Expression System: Secretion of Active Calf Chymosin from the Filamentous Fungus *Trichoderma reesei*. Nat Biotechnol. 1989 Jun 1;7(6):596–603.

51. Herrera-Estrella A, Goldman GH, Montagu M Van. Notes High-efficiency transformation system for the biocontrol agents, *Trichoderma* spp. Mol Microbiol. 1990 May 27;4(5):839–43.

52. Zhong YH, Wang XL, Wang TH, Jiang Q. *Agrobacterium*-mediated transformation (AMT) of *Trichoderma reesei* as an efficient tool for random insertional mutagenesis. Appl Microbiol Biotechnol. 2007 Jan;73(6):1348–54.

53. Goldman GH, Van Montagu M, Herrera-Estrella A. Transformation of *Trichoderma harzianum* by high-voltage electric pulse. Curr Genet. 1990 Feb;17(2):169–74.

54. Jinek M, Chylinski K, Fonfara I, Hauer M, Doudna JA, Charpentier E. A Programmable Dual-RNA–Guided DNA Endonuclease in Adaptive Bacterial Immunity. Science (1979). 2012 Aug 17;337(6096):816–21.

55. Rantasalo A, Vitikainen M, Paasikallio T, Jäntti J, Landowski CP, Mojzita D. Novel genetic tools that enable highly pure protein production in *Trichoderma reesei*. Sci Rep. 2019 Mar 22;9(1):5032.

56. Xu Q, Himmel ME, Singh A. Chapter 11: Production of Ethanol from Engineered *Trichoderma reesei*. In: Eckert CA, Trinh CT, editors. Direct Microbial Conversion of Biomass to Advanced Biofuels [Internet]. Elsevier; 2015. p. 197–208. Available from: http://www.scopus.com/inward/record.url?scp=85054698306&partnerID=8YFLogxK

57. Gusakov A V. Alternatives to *Trichoderma reesei* in biofuel production. Trends Biotechnol. 2011 Sep;29(9):419–25.

58. Hinterdobler W, Li G, Spiegel K, Basyouni-Khamis S, Gorfer M, Schmoll M. *Trichoderma reesei* Isolated From Austrian Soil With High Potential for Biotechnological Application. Front Microbiol. 2021 Jan 28;12.

59. Ciobanu M, Rusănescu CO, Dinculoiu RL. The Use of a *Trichoderma reesei* Culture for the Hydrolysis of Wheat Straw to Obtain Bioethanol. Processes. 2024 Nov 22;12(12):2625.

60. Lovén J, Orlando DA, Sigova AA, Lin CY, Rahl PB, Burge CB, et al. Revisiting global gene expression analysis. Cell. 2012 Oct 26;151(3):476–82.

61. Singh KP, Miaskowski C, Dhruva AA, Flowers E, Kober KM. Mechanisms and Measurement of Changes in Gene Expression. Biol Res Nurs. 2018 Jul;20(4):369–82.

62. Ma YJ, Dissen GA, Rage F, Ojeda SR. RNase Protection Assay. Methods. 1996 Dec;10(3):273–8.

63. Freeman WM, Robertson DJ, Vrana KE. Fundamentals of DNA Hybridization Arrays for Gene Expression Analysis. Biotechniques. 2000 Nov 29;29(5):1042–55.

64. Alberts B, Johnson A, Lewis J. Studying Gene Expression and Function. In: Molecular Biology of the Cell [Internet]. 4th edition. New York: Garland Science; 2002 [cited 2025 Jan 10]. Available from: https://www.ncbi.nlm.nih.gov/books/NBK26818/

65. Kukurba KR, Montgomery SB. RNA Sequencing and Analysis. Cold Spring Harb Protoc. 2015 Apr 13;2015(11):951–69.

66. Corchete LA, Rojas EA, Alonso-López D, De Las Rivas J, Gutiérrez NC, Burguillo FJ. Systematic comparison and assessment of RNA-seq procedures for gene expression quantitative analysis. Sci Rep. 2020 Nov 12;10(1):19737.

67. Kukurba KR, Montgomery SB. RNA Sequencing and Analysis. Cold Spring Harb Protoc. 2015 Apr 13;2015(11):951–69.

68. Saiki RK, Scharf S, Faloona F, Mullis KB, Horn GT, Erlich HA, et al. Enzymatic amplification of beta-globin genomic sequences and restriction site analysis for diagnosis of sickle cell anemia. Science. 1985;230(4732):1350–4.

69. Garibyan L, Avashia N. Polymerase chain reaction. J Invest Dermatol. 2013 Mar;133(3):1–4.

70. Enzoklop. Enzoklop, CC BY-SA 3.0 (https://creativecommons.org/licenses/by-sa/3.0), via Wikimedia Commons. [cited 2025 Jan 2]. Schematic drawing of the PCR cycle. Available from: https://commons.wikimedia.org/wiki/File:Polymerase_chain_reaction.svg

71. Saiki RK, Scharf S, Faloona F, Mullis KB, Horn GT, Erlich HA, et al. Enzymatic Amplification of β-Globin Genomic Sequences and Restriction Site Analysis for Diagnosis of Sickle Cell Anemia. Science (1979). 1985 Dec 20;230(4732):1350–4.

72. Lawyer FC, Stoffel S, Saiki RK, Chang SY, Landre PA, Abramson RD, et al. High-level expression, purification, and enzymatic characterization of full-length *Thermus aquaticus* DNA polymerase and a truncated form deficient in 5' to 3' exonuclease activity. Genome Res. 1993 May;2(4):275–87.

73. Picard V, Ersdal-Badju E, Lu A, Bock SC. A rapid and efficient one-tube PCR-based mutagenesis technique using *Pfu* DNA polymerase. Nucleic Acids Res. 1994;22(13):2587–91.

74. Kong H, Kucera RB, Jack WE. Characterization of a DNA polymerase from the hyperthermophile archaea *Thermococcus litoralis*. Vent DNA polymerase, steady state kinetics, thermal stability, processivity, strand displacement, and exonuclease activities. Journal of Biological Chemistry. 1993 Jan;268(3):1965–75.

75. Vigneault F, Drouin R. Optimal conditions and specific characteristics of *Vent* exo– DNA polymerase in ligation-mediated polymerase chain reaction protocols. Biochemistry and Cell Biology. 2005 Apr 1;83(2):147–65.

76. Lorenz TC. Polymerase Chain Reaction: Basic Protocol Plus Troubleshooting and Optimization Strategies. Journal of Visualized Experiments. 2012 May 22;(63).

77. Buell GN, Wickens MP, Payvar F, Schimke RT. Synthesis of full length cDNAs from four partially purified oviduct mRNAs. Journal of Biological Chemistry. 1978 Apr;253(7):2471–82.

78. Heid CA, Stevens J, Livak KJ, Williams PM. Real time quantitative PCR. Genome Res. 1996 Oct;6(10):986–94.

79. Orlando C, Pinzani P, Pazzagli M. Developments in Quantitative PCR. cclm. 1998 May 1;36(5):255–69.

80. Lorkowski S, Cullen P. Analysing Gene Expression. Lorkowski S, Cullen P, editors. Wiley; 2002.

81. Kozera B, Rapacz M. Reference genes in real-time PCR. J Appl Genet. 2013 Nov;54(4):391–406.

82. Bustin SA, Benes V, Garson JA, Hellemans J, Huggett J, Kubista M, et al. The MIQE Guidelines: Minimum Information for Publication of Quantitative Real-Time PCR Experiments. Clin Chem. 2009 Apr 1;55(4):611–22.

83. Kubista M, Andrade JM, Bengtsson M, Forootan A, Jonák J, Lind K, et al. The real-time polymerase chain reaction. Mol Aspects Med. 2006;27(2–3):95–125.

84. Adams G. A beginner's guide to RT-PCR, qPCR and RT-qPCR. Biochem (Lond). 2020 Jun 23;42(3):48–53.

85. Freitas FCP, Depintor TS, Agostini LT, Luna-Lucena D, Nunes FMF, Bitondi MMG, et al. Evaluation of reference genes for gene expression analysis by real-time quantitative PCR (qPCR) in three stingless bee species (Hymenoptera: Apidae: Meliponini). Sci Rep. 2019 Nov 27;9(1):17692.

86. Chervoneva I, Li Y, Schulz S, Croker S, Wilson C, Waldman SA, et al. Selection of optimal reference genes for normalization in quantitative RT-PCR. BMC Bioinformatics. 2010 May 14;11:253.

87. de Jonge HJM, Fehrmann RSN, de Bont ESJM, Hofstra RMW, Gerbens F, Kamps WA, et al. Evidence Based Selection of Housekeeping Genes. PLoS One. 2007 Sep 19;2(9):e898.

88. Archer M, Xu J. Current Practices for Reference Gene Selection in RT-qPCR of *Aspergillus*: Outlook and Recommendations for the Future. Genes (Basel). 2021 Jun 24;12(7):960.

89. Hellemans J, Mortier G, De Paepe A, Speleman F, Vandesompele J. qBase relative quantification framework and software for management and automated analysis of real-time quantitative PCR data. Genome Biol. 2007;8(2):R19.

90. Silver N, Best S, Jiang J, Thein SL. Selection of housekeeping genes for gene expression studies in human reticulocytes using real-time PCR. BMC Mol Biol. 2006 Dec 6;7(1):33.

91. Pfaffl MW, Tichopad A, Prgomet C, Neuvians TP. Determination of stable housekeeping genes, differentially regulated target genes and sample integrity: BestKeeper – Excel-based tool using pair-wise correlations. Biotechnol Lett. 2004 Mar;26(6):509–15.

92. Andersen CL, Jensen JL, Ørntoft TF. Normalization of Real-Time Quantitative Reverse Transcription-PCR Data: A Model-Based Variance Estimation Approach to Identify

Genes Suited for Normalization, Applied to Bladder and Colon Cancer Data Sets. Cancer Res. 2004 Aug 1;64(15):5245–50.

93. Vandesompele J, De Preter K, Pattyn F, Poppe B, Van Roy N, De Paepe A, et al. Accurate normalization of real-time quantitative RT-PCR data by geometric averaging of multiple internal control genes. Genome Biol. 2002 Jun 18;3(7):research0034.1.

94. Xie F, Wang J, Zhang B. RefFinder: a web-based tool for comprehensively analyzing and identifying reference genes. Funct Integr Genomics. 2023 Jun 15;23(2):125.

95. Zhou Z, Cong P, Tian Y, Zhu Y. Using RNA-seq data to select reference genes for normalizing gene expression in apple roots. PLoS One. 2017;12(9):e0185288.

96. Tao Y, van Peer AF, Huang Q, Shao Y, Zhang L, Xie B, et al. Identification of novel and robust internal control genes from Volvariella volvacea that are suitable for RT-qPCR in filamentous fungi. Sci Rep. 2016 Jul 12;6(1):29236.

97. Fu N, Li J, Wang M, Ren L, Zong S, Luo Y. Identification and Validation of Reference Genes for Gene Expression Analysis in Different Development Stages of *Amylostereum areolatum*. Front Microbiol. 2022 Jan 12;12.

98. Besleaga M, Vignolle GA, Kopp J, Spadiut O, Mach RL, Mach-Aigner AR, et al. Evaluation of reference genes for transcript analyses in Komagataella phaffii (Pichia pastoris). Fungal Biol Biotechnol [Internet]. 2023;10(1):7. Available from: C:\Users\juriy\Documents\Citavi 6\Projects\ICG\Citavi Attachments\Besleaga, Vignolle et al. 2023 - Evaluation of reference genes.pdf

99. Besleaga M, Vignolle GA, Kopp J, Spadiut O, Mach RL, Mach-Aigner AR, et al. Evaluation of reference genes for transcript analyses in *Komagataella phaffii* (*Pichia pastoris*). Fungal Biol Biotechnol. 2023 Mar 29;10(1):7.

100. Steiger MG, Mach RL, Mach-Aigner AR. An accurate normalization strategy for RT-qPCR in *Hypocrea jecorina* (*Trichoderma reesei*). J Biotechnol. 2010 Jan 1;145(1):30–7.

101. Institute EB. SRA FTP site [Internet]. 2024. Available from: https://ftp.sra.ebi.ac.uk/

102. Kim Lab at UT Southwestern Medical Center. HISAT2 - Graph-based alignment of next generation sequencing reads to a population of genomes [Internet]. 2024 [cited 2024 Dec 17]. Available from: https://daehwankimlab.github.io/hisat2/

103. Samtools - organisation for next-generation sequencing developers. SAMtools [Internet]. 2024 [cited 2024 Jul 12]. Available from: https://www.htslib.org/

104. Danecek P, Bonfield JK, Liddle J, Marshall J, Ohan V, Pollard MO, et al. Twelve years of SAMtools and BCFtools. Gigascience. 2021 Jan 29;10(2).

105. featureCounts: a ultrafast and accurate read summarization program [Internet]. [cited 2024 Dec 17]. Available from: https://subread.sourceforge.net/featureCounts.html

106. Liao Y, Smyth GK, Shi W. featureCounts: an efficient general purpose program for assigning sequence reads to genomic features. Bioinformatics. 2014 Apr 1;30(7):923–30.

107. Love Lab (UNC-Chapel Hill). DESeq2 - Differential gene expression analysis based on the negative binomial distribution [Internet]. [cited 2024 Dec 17]. Available from: https://github.com/thelovelab/DESeq2

108. Geo Pertea. gffRead - GFF/GTF utility providing format conversions, region filtering, FASTA sequence extraction and more [Internet]. 2021 [cited 2024 Dec 17]. Available from: https://github.com/gpertea/gffread

109. Altschul SF, Gish W, Miller W, Myers EW, Lipman DJ. Basic local alignment search tool. J Mol Biol. 1990 Oct;215(3):403–10.

110. Okonechnikov K, Golosova O, Fursov M. Unipro UGENE: a unified bioinformatics toolkit. Bioinformatics. 2012 Apr 15;28(8):1166–7.

111. Hernández-Plaza A, Szklarczyk D, Botas J, Cantalapiedra CP, Giner-Lamia J, Mende DR, et al. eggNOG 6.0: enabling comparative genomics across 12 535 organisms. Nucleic Acids Res. 2023 Jan 6;51(D1):D389–94.

112. Guo L, Han L, Yang L, Zeng H, Fan D, Zhu Y, et al. Genome and transcriptome analysis of the fungal pathogen *Fusarium oxysporum f. sp. cubense* causing banana vascular wilt disease. PLoS One. 2014;9(4):e95543.

113. Wendler F, Gillingham AK, Sinka R, Rosa-Ferreira C, Gordon DE, Franch-Marro X, et al. A genome-wide RNA interference screen identifies two novel components of the metazoan secretory pathway. EMBO J. 2010 Jan 20;29(2):304–14.

114. Shih SC, Prag G, Francis SA, Sutanto MA, Hurley JH, Hicke L. A ubiquitin-binding motif required for intramolecular monoubiquitylation, the CUE domain. EMBO J. 2003 Mar 17;22(6):1273–81.

115. Huang DT, Walden H, Duda D, Schulman BA. Ubiquitin-like protein activation. Oncogene. 2004 Mar 15;23(11):1958–71.

116. Kwon JY, Choi YH, Lee MW, Yu JH, Shin KS. The MYST Family Histone Acetyltransferase SasC Governs Diverse Biological Processes in *Aspergillus fumigatus*. Cells. 2023 Nov 16;12(22).

117. East China University of Science and Technology. NCBI Sequence Read Archive (SRA). 2023 [cited 2024 Jul 7]. Transcriptional profile of the *Trichoderma reesei* OEtre105752 mutant. Available from: https://www.ncbi.nlm.nih.gov/bioproject/PRJNA948159

118. East China University of Science and Technology. NCBI Sequence Read Archive (SRA). 2019 [cited 2024 Jul 7]. Transcriptional profile of the *Trichoderma reesei* ace3 deletion mutant cultured in the presence of lactose. Available from: https://www.ncbi.nlm.nih.gov/bioproject/PRJNA526091

119. Brazilian Bioethanol Science and Technology Laboratory (CTBE). NCBI Sequence Read Archive (SRA). 2017 [cited 2024 Jul 7]. Global Transcriptome and Gene Regulatory Network of MAPK Signaling Pathway in *Trichoderma reesei* During Sugarcane Bagasse Degradation. Available from: https://www.ncbi.nlm.nih.gov/bioproject/PRJNA392276

120. Bioresources H and EAAI of T. NCBI Sequence Read Archive (SRA). 2018 [cited 2024 Jul 7]. YPR2 is a light dependent regulator of carbon and secondary metabolism in *Trichoderma reesei*. Available from: https://www.ncbi.nlm.nih.gov/bioproject/PRJNA488233

121. East China University of Science and Technology. NCBI Sequence Read Archive (SRA). 2018 [cited 2024 Jul 7]. Comparing the two transcriptomes of *Trichoderma reesei* QM6a cultured with 0 and 1% DMF in liquid MM containing 1% Avicel as the sole carbon source. Available from: https://www.ncbi.nlm.nih.gov/bioproject/PRJNA510366

122. Working Group Mattanovich D of BU of NR and LS. NCBI Sequence Read Archive (SRA). 2019 [cited 2024 Jul 7]. RNAseq analysis of *Trichoderma reesei* QM6a and Δace1 transferred to MA medium containing 1% D-mannitol as carbon source. Available from: https://www.ncbi.nlm.nih.gov/bioproject/PRJNA528215

123. DOE Joint Genome Institute (JGI). NCBI Sequence Read Archive (SRA). 2021 [cited 2025 Jul 7]. *Trichoderma reesei* QM6a Crude Substrate Gene Expression Profiling. Available from: https://www.ncbi.nlm.nih.gov/bioproject/PRJNA695932

124. Alharake J, Bidard F, Aouam T, Sénamaud-Beaufort C, Margeot A, Heiss-Blanquet S. Effect of the res2 transcription factor gene deletion on protein secretion and stress

response in the hyperproducer strain *Trichoderma reesei* Rut-C30. BMC Microbiol. 2023 Nov 30;23(1):374.

125. Genomic Core Facility I. NCBI Sequence Read Archive (SRA). 2023 [cited 2024 Jul 7]. Effect of the res-2 transcription factor gene deletion on protein secretion and stress response in the hyperproducer strain *Trichoderma reesei* Rut-C30. Available from: https://www.ncbi.nlm.nih.gov/bioproject/PRJNA977675

126. Borin GP, Sanchez CC, de Souza AP, de Santana ES, de Souza AT, Paes Leme AF, et al. Comparative Secretome Analysis of *Trichoderma reesei* and *Aspergillus niger* during Growth on Sugarcane Biomass. PLoS One. 2015;10(6):e0129275.

127. Laboratorio Nacional de Ciencia e Tecnologia do Bi. NCBI Sequence Read Archive (SRA). 2016 [cited 2024 Jul 7]. Comparative Secretome Analysis of *Trichoderma reesei* and *Aspergillus niger* during Growth on Sugarcane Biomass. Available from: https://www.ncbi.nlm.nih.gov/bioproject/PRJNA350272

128. East China University of Science and Technology. NCBI Sequence Read Archive (SRA). 2023 [cited 2024 Jul 7]. The effect of 3 mM Zn2+ on cellulase production in *Trichoderma reesei* Rut-C30 with 1% Avicel as the sole carbon source. Available from: https://www.ncbi.nlm.nih.gov/bioproject/PRJNA923496

129. Schilling lab P and MBU of M. NCBI Sequence Read Archive (SRA). 2024 [cited 2025 Jul 7]. Melanization of fungal necromass drives the upregulation of multiple chitinase, protease, and laccase genes when being degraded by *Trichoderma reesei*. Available from: https://www.ncbi.nlm.nih.gov/bioproject/PRJNA1097855

9 Annex

9.1 RNA-seq data of *T. reesei* QM6a

Table 9: Specifics of RNA-Seq data of the strain QM6a used in the bioinformatics analysis

Run	SRA Study	Bases	Size	Platform	Condition	Reference
SRR23952272	SRP429031	7,6 G	2,1 Gb	Illumina NovaSeq 6000	growth on glucose repl. 1	(117)
SRR23952273	SRP429031	6,8 G	1,9 Gb	Illumina NovaSeq 6000	growth on glucose repl. 2	
SRR8698740	SRP187914	7 G	2,9 Gb	Illumina HiSeq 2000	2 % lactose (transfer after 12 h) - repl. 1	(118)
SRR8698741	SRP187914	7,8 G	3,2 Gb	Illumina HiSeq 2000	2 % lactose (transfer after 12 h) - repl. 2	
SRR5765024	SRP110683	2,9 G	2 Gb	Illumina HiSeq 2500	1 % sugarcane bagasse 48 h - repl.1	(119)
SRR5765025	SRP110683	3 G	2 Gb	Illumina HiSeq 2500	1 % sugarcane bagasse 48 h - repl.2	
SRR5765030	SRP110683	3,2 G	2,1 Gb	Illumina HiSeq 2500	1 % sugarcane bagasse (transfer from 1 % glycerol) - repl.1	
SRR5765031	SRP110683	4 G	2,7 Gb	Illumina HiSeq 2500	1 % sugarcane bagasse (transfer from 1 % glycerol) - repl.2	
SRR7761289	SRP159003	2,8 G	1,8 Gb	Illumina HiSeq 2000	Mandels Andreotti + 1 % cellulose in constant light - repl.1	(120)
SRR7761290	SRP159003	2,7 G	1,7 Gb	Illumina HiSeq 2000	Mandels Andreotti + 1 % cellulose in constant light - repl.2	
SRR7761293	SRP159003	2,7 G	1,7 Gb	Illumina HiSeq 2000	Mandels Andreotti + 1 % cellulose in constant dark - repl.1	
SRR7761294	SRP159003	2,6 G	1,6 Gb	Illumina HiSeq 2000	Mandels Andreotti + 1 % cellulose in constant dark - repl.2	
SRR8329346	SRP173612	7,5 G	2,7 Gb	Illumina HiSeq X Ten	MM with 1 % Avicell 48 h - repl.1	(121)
SRR8329347	SRP173612	6,9 G	2,4 Gb	Illumina HiSeq X Ten	MM with 1 % Avicell 48 h - repl.2	
SRR8329344	SRP173612	7,6 G	2,7 Gb	Illumina HiSeq X Ten	MM with 1 % Avicell + 1 % DMF 48 h - repl.1	
SRR8329345	SRP173612	7,1 G	2,5 Gb	Illumina HiSeq X Ten	MM with 1 % Avicell + 1 % DMF 48 h - repl.2	
SRR8756161	SRP188940	882,3 M	368 Mb	Illumina NextSeq 500	24 h on Mandels Andreotti with glucose - transfer for 3 h to 1 % D-Mannitol - repl.1	(122)
SRR8756162	SRP188940	738,7 M	306,6 Mb	Illumina NextSeq 500	24 h on Mandels Andreotti with glucose - transfer for 3 h to 1 % D-Mannitol - repl.2	
SRR25252694	SRP448956	2,7 G	908,6 Mb	Illumina NovaSeq 6000	1x MA with 1 % corn stover – 4 h transfer - repl.1	(123)
SRR25252695	SRP448955	2,7 G	908 Mb	Illumina NovaSeq 6000	1x MA with 1 % corn stover – 4 h transfer - repl.2	
SRR19551435	SRP378722	5,9 G	1,7 Gb	Illumina NovaSeq 6000	1x MA + 25 mM D-glucuronic acid – 4 h transfer - repl.1	
SRR19551437	SRP378720	4,5 G	1,3 Gb	Illumina NovaSeq 6000	1x MA + 25 mM D-glucuronic acid – 4 h transfer - repl.2	

SRR19551421	SRP378737	6,7 G	2 Gb	Illumina NovaSeq 6000	1x MA + 25 mM L-arabinose – 4 h transfer - repl.1
SRR19551434	SRP378723	6,9 G	2,1 Gb	Illumina NovaSeq 6000	1x MA + 25 mM L-arabinose – 4 h transfer - repl.2
SRR19551432	SRP378725	5,3 G	1,6 Gb	Illumina NovaSeq 6000	1x MA + 25 mM L-rhamnose – 4 h transfer - repl.1
SRR19551433	SRP378724	4,9 G	1,5 Gb	Illumina NovaSeq 6000	1x MA + 25 mM L-rhamnose – 4 h transfer - repl.2
SRR19551429	SRP378728	6,8 G	2 Gb	Illumina NovaSeq 6000	1x MA + 25 mM D-galacturonic acid – 4 h transfer - repl.1
SRR19551431	SRP378726	6,9 G	2 Gb	Illumina NovaSeq 6000	1x MA + 25 mM D-galacturonic acid – 4 h transfer - repl.2
SRR19551420	SRP378736	6,1 G	1,8 Gb	Illumina NovaSeq 6000	1x MA + 25 mM D-xylose – 4 h transfer - repl.1
SRR19551428	SRP378729	7,4 G	2,2 Gb	Illumina NovaSeq 6000	1x MA + 25 mM D-xylose – 4 h transfer - repl.2
SRR19551424	SRP378733	5,1 G	1,5 Gb	Illumina NovaSeq 6000	1x MA + 25 mM D-mannose – 4 h transfer - repl.1
SRR19551425	SRP378732	3,9 G	1,1 Gb	Illumina NovaSeq 6000	1x MA + 25 mM D-mannose – 4 h transfer - repl.2
SRR19551413	SRP378744	4,5 G	1,2 Gb	Illumina NovaSeq 6000	1x MA + 25 mM D-galactose – 4 h transfer - repl.1
SRR19551423	SRP378734	4,8 G	1,4 Gb	Illumina NovaSeq 6000	1x MA + 25 mM D-galactose – 4 h transfer - repl.2
SRR19551416	SRP378741	4,2 G	1,2 Gb	Illumina NovaSeq 6000	1x MA + 25 mM D-fructose – 4 h transfer - repl.1
SRR19551418	SRP378739	4,2 G	1,2 Gb	Illumina NovaSeq 6000	1x MA + 25 mM D-fructose – 4 h transfer - repl.2
SRR19551414	SRP378743	5,2 G	1,5 Gb	Illumina NovaSeq 6000	1x MA + 25 mM D-glucose – 4 h transfer - repl.1
SRR19551415	SRP378742	6,6 G	1,8 Gb	Illumina NovaSeq 6000	1x MA + 25 mM D-glucose – 4 h transfer - repl.2

9.2 RNA-seq data of *T. reesei* Rut-C30

Table 10: Specifics of RNA-Seq data of the strain Rut-C30 used in the bioinformatics analysis

Run	SRA Study	Bases	Size	Platform	Condition	Reference
SRR24768099	SRP440257	6,3 G	2 Gb	Illumina NextSeq 2000	Fed-batch with lactose + 10 mM DTT for 2 h - repl.1	(124,125)
SRR24768104	SRP440257	5,9 G	1,9 Gb	Illumina NextSeq 2000	Fed-batch with lactose + 10 mM DTT for 2 h - repl.2	
SRR24768100	SRP440257	4,6 G	1,4 Gb	Illumina NextSeq 2000	Fed-batch with lactose - repl.1	
SRR24768103	SRP440257	5,2 G	1,6 Gb	Illumina NextSeq 2000	Fed-batch with lactose - repl.2	
SRR24768101	SRP440257	5,3 G	1,6 Gb	Illumina NextSeq 2000	Fed-batch with glucose + 10 mM DTT for 2 h - repl.1	
SRR24768102	SRP440257	5,7 G	1,7 Gb	Illumina NextSeq 2000	Fed-batch with glucose + 10 mM DTT for 2 h - repl.2	
SRR24768105	SRP440257	4,7 G	1,4 Gb	Illumina NextSeq 2000	Fed-batch with glucose - repl.1	
SRR24768106	SRP440257	4,5 G	1,3 Gb	Illumina NextSeq 2000	Fed-batch with glucose - repl.2	
SRR4446960	SRP091982	2,4 G	1,6 Gb	Illumina HiSeq 2000	BCM with 1 % fructose 48 h + 24 h - rep.1	(126,127)
SRR4446961	SRP091982	2,5 G	1,7 Gb	Illumina HiSeq 2000	BCM with 1 % fructose 48 h + 24 h - rep.2	
SRR4446958	SRP091982	2,5 G	1,7 Gb	Illumina HiSeq 2000	BCM with 1 % fructose 48 h - transfer to 0,5 % SEB 24 h - rep.1	
SRR4446959	SRP091982	2,5 G	1,7 Gb	Illumina HiSeq 2000	BCM with 1 % fructose 48 h - transfer to 0,5 % SEB 24 h - rep.2	
SRR4446955	SRP091982	2,3 G	1,6 Gb	Illumina HiSeq 2000	BCM with 1 % fructose 48 h - transfer to 0,5 % SEB 12 h - rep.1	
SRR4446956	SRP091982	2,7 G	1,8 Gb	Illumina HiSeq 2000	BCM with 1 % fructose 48 h - transfer to 0,5 % SEB 12 h - rep.2	
SRR4446953	SRP091982	2,5 G	1,7 Gb	Illumina HiSeq 2000	BCM with 1 % fructose 48 h - transfer to 0,5 % SEB 6 h - rep.1	
SRR4446954	SRP091982	2,4 G	1,7 Gb	Illumina HiSeq 2000	BCM with 1 % fructose 48 h - transfer to 0,5 % SEB 6 h - rep.2	
SRR23088649	SRP417642	6,6 G	1,9 Gb	Illumina NovaSeq 6000	1 % Avicell 48 h - repl.1	(128)
SRR23088650	SRP417642	7,2 G	2,1 Gb	Illumina NovaSeq 6000	1 % Avicell 48 h - repl.2	
SRR23088646	SRP417642	8,3 G	2,4 Gb	Illumina NovaSeq 6000	1 % Avicell 48 h + 3 mM Zn^{2+} - repl.1	
SRR23088647	SRP417642	7,1 G	2 Gb	Illumina NovaSeq 6000	1 % Avicell 48 h + 3 mM Zn^{2+} - repl.2	
SRR28595945	SRP500486	7,9 G	2,4 Gb	Illumina HiSeq 4000	high-melanin necromass from *Hyaloscypha bicolor* - repl.1	(129)
SRR28595946	SRP500486	8,5 G	2,6 Gb	Illumina HiSeq 4000	high-melanin necromass from *Hyaloscypha bicolor* - repl.2	
SRR28595948	SRP500486	8 G	2,5 Gb	Illumina HiSeq 4000	low-melanin necromass from *Hyaloscypha bicolor* - repl.1	
SRR28595949	SRP500486	8,5 G	2,6 Gb	Illumina HiSeq 4000	low-melanin necromass from *Hyaloscypha bicolor* - repl.2	

9.3 Code used for extraction of count data

This section contains exemplary commands used in the Terminal of Debian 12 to extract count information from the RNA-seq files.

Indexing of genomes for further use in HISAT2:

```
hisat2-build genome.fa genome
```

Writing a SAM file from paired end RNA-seq files:

```
hisat2 -x genome -1 sample_R1.fastq.gz -2 sample_R2.fastq.gz -S output.sam
```

Writing a SAM file from single-end RNA-seq file:

```
hisat2 -x genome_index -U sample.fastq.gz -S output.sam
```

Conversion from SAM to BAM format via SAMtools:

```
samtools sort -l 9 -o output.bam -@ 4 output.sam
```

Extraction of raw counts from the SAM file:

```
featureCounts -p -t exon -g gene_id -a annotation.gtf -o output.txt output.bam
```

9.4 Code used in DESeq2

This chapter contains an exemplary code used in R to receive normalized counts from raw counts with the help of the package DESeq2. This code is reduced to only two conditions in duplicates and output folder information is not displayed.

```
if (!requireNamespace("BiocManager", quietly = TRUE)) {
  install.packages("BiocManager")
}
BiocManager::install("DESeq2")
BiocManager::install("EnhancedVolcano")

install.packages("writexl")

library(writexl)
library(DESeq2)
library(EnhancedVolcano)

cond1_1 <- read.table("C:/---/cond1_1.txt", header = TRUE, sep =
"\t", stringsAsFactors = FALSE)
cond1_2 <- read.table("C:/---/cond1_2.txt", header = TRUE, sep =
"\t", stringsAsFactors = FALSE)
cond2_1 <- read.table("C:/---/cond2_1.txt", header = TRUE, sep =
"\t", stringsAsFactors = FALSE)
cond2_2 <- read.table("C:/---/cond2_2.txt", header = TRUE, sep =
"\t", stringsAsFactors = FALSE)

countData1_cond1_1 <- cond1_1[, 7:ncol(cond1_2)]
countData1_cond1_2 <- cond1_2[, 7:ncol(cond1_2)]
countData2_cond2_1 <- cond2_1[, 7:ncol(cond2_1)]
countData2_cond2_2 <- cond2_1[, 7:ncol(cond2_2)]

countData1_cond1_1 <- as.data.frame(countData1_cond1_1)
countData1_cond1_2 <- as.data.frame(countData1_cond1_2)
countData2_cond2_1 <- as.data.frame(countData2_cond2_1)
countData2_cond2_2 <- as.data.frame(countData2_cond2_2)

rownames(countData1_cond1_1) <- cond1_1$Geneid
rownames(countData1_cond1_2) <- cond1_2$Geneid
rownames(countData2_cond2_1) <- cond2_1$Geneid
rownames(countData2_cond2_2) <- cond2_2$Geneid

countData <- cbind(countData1_cond1_1, countData1_cond1_2,
countData2_cond2_1, countData2_cond2_2)
colnames(countData) <- c("Condition1 1", "Condition1 2")

ncol(countData)

sampleInfo <- data.frame(
  row.names = colnames(countData),
  condition = factor(rep(c("Condition1", "Condition2"), each = 2)),
  replicate = factor(rep(c("Rep1", "Rep2"), 2))
)
```

```
dds <- DESeqDataSetFromMatrix(countData = countData, colData =
sampleInfo, design = ~ condition)
dds <- estimateSizeFactors(dds)
normalized_counts <- counts(dds, normalized=TRUE)
normalized_counts_df <- as.data.frame(normalized_counts)
normalized_counts_df$GeneID <- rownames(normalized_counts_df)
normalized_counts_df <- normalized_counts_df[,
c(ncol(normalized_counts_df), 1:(ncol(normalized_counts_df) - 1))]

write_xlsx(normalized_counts_df, "C:/---/normalized_counts.xlsx")
```

9.5 Primer sequences

Table 11 contains all seven sets of primers used in the qPCR analysis with all four strains of *T. reesei*.

Table 11: Primers used in the qPCR.

Primer	Sequence (5' → 3')	Product length [bp]	Melting temperature T_m [°C]
act1 forward	TGAGAGCGGTGGTATCCACG	103	55.9
act1 reverse	GGTACCACCAGACATGACAATGTTG		57.7
sar1 forward	TGGATCGTCAACTGGTTCTACGA	115	55.3
sar1 reverse	GCATGTGTAGCAACGTGGTCTTT		55.3
Bzip forward	GGCCTTTCTTTGAGCAGTGATG	92	54.8
Bzip reverse	AGCTGCCCTTTGTTGTTGTC		51.8
traff forward	TATGCGAATGAGCCGATTCC	78	51.8
traff reverse	AACGTCCAGCTTCACATTGG		51.8
CUE forward	GCGTAATCAAGGCGGTTCTG	108	53.8
CUE reverse	TGTTTTGCGGCTCGTTCTTG		51.8
Ubi1 forward	TCAAATGCGGGCGACAAAAG	112	51.8
Ubi1 reverse	TGTTGACCGGATGTTTGCAC		51.8
SAS3 forward	ATCGCGTGCTGTACATTTGC	91	51.8
SAS3 reverse	TGTTTCGCAGCGCATTTGAG		51.8

9.6 Ct-values from RT-qPCR analysis

Table 12: Ct-values obtained via RT-qPCR analysis

				Ct-values						
Strain	**C-source**	**Time-point**	**Dupli-cate**	*sar1*	*act1*	*bzip*	*traff*	*cue*	*ubi1*	*sas3*
QM6a	Cellulose	120	1	19,80	19,56	18,50	19,55	18,83	19,48	20,59
QM6a	Cellulose	120	2	21,45	21,80	18,51	19,60	19,83	19,81	21,29
QM6a	Cellulose	48	1	18,46	17,35	19,26	20,74	19,57	20,59	22,09
QM6a	Cellulose	48	2	18,78	18,04	18,59	19,79	18,91	19,83	21,01
QM6a	DTT	6	1	19,84	22,19	19,97	22,40	19,60	21,08	21,66
QM6a	DTT	6	2	20,51	21,92	19,60	21,75	19,69	19,97	21,04
QM6a	DTT	48	1	21,38	23,29	18,35	19,05	18,97	18,51	19,37
QM6a	DTT	48	2	21,90	24,03	18,51	19,34	19,66	18,63	19,77
QM6a	Glucose	36	1	23,96	22,87	17,18	18,04	17,38	17,36	18,40
QM6a	Glucose	36	2	23,95	22,68	17,27	17,97	17,45	17,42	18,45
QM6a	Glucose	84	1	23,44	22,54	18,41	19,24	18,89	19,10	20,35
QM6a	Glucose	84	2	24,87	24,10	18,58	19,61	19,75	19,62	21,09
QM6a	Glycerin	84	1	23,83	24,88	21,37	21,98	22,19	20,77	22,01
QM6a	Glycerin	84	2	24,10	25,60	20,07	20,96	21,28	19,59	21,09
QM6a	Glycerin	24	1	17,08	16,81	18,72	19,52	17,93	19,26	20,89
QM6a	Glycerin	24	2	17,26	16,08	19,02	19,69	17,97	19,26	20,87
QM6a	Induced	96	1	21,90	21,94	20,88	22,17	21,98	21,46	22,97
QM6a	Induced	96	2	22,97	23,23	20,83	21,93	22,22	21,25	22,53
QM6a	Induced	48	1	19,44	18,40	19,08	20,11	19,42	18,67	20,00
QM6a	Induced	48	2	20,19	19,13	19,47	20,66	19,60	18,67	19,91
QM6a	Lactose	96	2	20,81	20,13	19,03	20,06	19,99	18,63	19,68
QM6a	Lactose	96	1	21,55	20,33	17,26	18,30	18,19	16,47	17,73
QM6a	Lactose	72	1	19,10	21,37	17,93	18,77	18,82	17,88	18,98
QM6a	Lactose	72	2	19,67	20,73	17,88	19,15	19,25	18,20	19,37
QM6a	NaCl	6	1	21,08	21,01	18,55	19,80	19,12	18,87	19,71
QM6a	NaCl	6	2	19,90	19,99	18,22	19,49	18,72	18,67	19,68
QM6a	NaCl	24	1	19,16	19,24	17,88	19,13	18,06	19,02	20,22
QM6a	NaCl	24	2	19,77	20,30	18,88	20,46	19,20	20,13	21,48
QM6a	Xylan	48	1	21,62	22,38	18,82	20,26	20,54	19,18	20,65
QM6a	Xylan	48	2	21,08	21,80	21,31	23,02	22,52	21,77	23,26
QM6a	Xylan	24	1	18,89	18,75	17,93	18,98	18,65	18,13	19,39
QM6a	Xylan	24	2	18,12	18,03	19,02	19,95	19,11	19,41	20,37
RUT-C30	Cellulose	120	1	20,66	20,73	18,80	19,76	19,23	19,65	20,87
RUT-C30	Cellulose	120	2	20,32	21,33	17,61	18,34	17,84	18,24	19,26
RUT-C30	Cellulose	48	1	17,77	17,36	18,60	19,68	18,88	19,85	21,13
RUT-C30	Cellulose	48	2	17,69	17,36	18,38	19,40	18,61	19,46	20,56
RUT-C30	DTT	6	1	23,88	22,19	19,67	21,70	21,20	20,22	21,43
RUT-C30	DTT	6	2	25,49	25,82	19,11	21,24	20,32	18,49	19,45
RUT-C30	DTT	48	1	20,53	19,97	20,81	22,24	20,11	21,38	22,54
RUT-C30	DTT	48	2	20,96	20,73	16,79	17,86	17,63	17,31	18,56
RUT-C30	Glucose	84	1	23,04	23,98	18,54	19,39	19,08	19,24	20,59

RUT-C30	Glucose	84	2	23,84	24,92	18,76	19,82	19,93	19,20	20,50
RUT-C30	Glucose	24	1	18,62	18,82	18,53	19,33	18,91	19,37	20,43
RUT-C30	Glucose	24	2	18,58	18,39	19,56	20,64	20,07	20,54	22,19
RUT-C30	Glycerin	36	1	20,50	19,42	17,84	18,60	18,13	17,10	17,99
RUT-C30	Glycerin	36	2	21,53	20,69	17,11	18,17	18,00	16,78	17,80
RUT-C30	Glycerin	84	1	18,87	20,41	18,36	19,58	19,02	19,29	20,40
RUT-C30	Glycerin	84	2	18,02	19,29	18,41	19,50	19,17	18,78	20,07
RUT-C30	Induced	96	1	23,87	23,57	23,27	24,17	23,71	21,46	22,97
RUT-C30	Induced	96	2	23,77	23,85	20,15	21,16	20,93	21,25	22,53
RUT-C30	Induced	48	1	19,92	20,05	20,18	21,39	21,40	18,67	21,46
RUT-C30	Induced	48	2	18,42	18,03	18,48	19,61	19,28	18,67	21,25
RUT-C30	Lactose	48	1	19,96	20,20	21,54	22,46	21,24	21,55	23,05
RUT-C30	Lactose	48	2	19,68	20,86	20,21	21,25	21,03	20,33	21,88
RUT-C30	Lactose	72	1	21,74	22,29	18,18	19,11	19,37	18,23	19,39
RUT-C30	Lactose	72	2	20,01	22,33	18,75	20,07	19,98	18,87	20,17
RUT-C30	NaCl	6	1	20,38	19,90	17,73	19,20	18,14	18,77	19,73
RUT-C30	NaCl	6	2	19,95	19,28	17,31	18,60	17,53	18,09	18,92
RUT-C30	NaCl	24	1	20,13	19,27	18,10	19,34	18,44	18,56	19,35
RUT-C30	NaCl	24	2	21,28	20,47	18,29	18,94	18,74	18,26	19,11
RUT-C30	Xylan	48	1	21,95	21,70	17,57	18,67	18,59	17,65	18,80
RUT-C30	Xylan	48	2	21,50	21,31	22,20	24,18	22,84	21,93	23,46
RUT-C30	Xylan	24	1	20,05	18,94	20,10	21,32	20,61	19,67	21,04
RUT-C30	Xylan	24	2	19,82	19,01	19,50	20,59	20,14	19,16	20,34
RL-P37	Cellulose	120	1	20,70	20,78	18,23	19,41	19,11	20,76	20,46
RL-P37	Cellulose	120	2	20,19	20,95	18,84	21,76	19,16	19,68	20,74
RL-P37	Cellulose	48	1	18,43	18,31	20,16	21,37	19,66	21,57	19,33
RL-P37	Cellulose	48	2	20,38	20,18	20,69	21,68	20,96	21,79	19,68
RL-P37	DTT	6	1	20,44	24,89	20,03	21,12	19,86	20,08	21,27
RL-P37	DTT	6	2	20,02	24,72	20,04	21,37	20,57	19,65	20,68
RL-P37	DTT	48	1	19,78	19,72	18,18	19,65	18,02	22,83	20,38
RL-P37	DTT	48	2	20,43	19,88	20,31	22,57	19,19	21,90	22,89
RL-P37	Glucose	24	1	19,19	18,96	18,67	19,70	19,32	19,60	20,86
RL-P37	Glucose	24	2	19,50	19,63	17,47	18,32	18,64	18,17	19,57
RL-P37	Glucose	84	1	19,90	21,85	18,26	19,30	19,38	19,22	20,43
RL-P37	Glucose	84	2	20,54	21,82	19,15	20,42	20,55	20,83	22,22
RL-P37	Glycerin	24	1	18,85	18,24	18,04	19,24	18,91	18,48	20,06
RL-P37	Glycerin	24	2	19,93	19,35	17,99	18,96	18,85	18,04	19,33
RL-P37	Glycerin	84	1	18,33	18,95	17,30	18,16	17,46	17,72	18,54
RL-P37	Glycerin	84	2	19,14	20,01	17,95	18,88	18,25	18,34	19,31
RL-P37	Induced	96	1	23,06	24,04	23,51	24,07	22,76	25,30	24,06
RL-P37	Induced	96	2	24,24	24,80	25,15	25,68	24,48	24,60	25,21
RL-P37	Induced	48	1	19,59	19,86	20,19	21,48	20,28	19,90	22,87
RL-P37	Induced	48	2	18,96	18,98	19,54	20,59	19,54	19,10	24,60
RL-P37	Lactose	72	1	21,86	22,25	18,41	19,47	18,79	18,46	19,68
RL-P37	Lactose	72	2	22,71	23,07	17,99	18,93	18,22	17,94	19,14
RL-P37	Lactose	48	1	19,42	19,69	17,44	18,25	17,94	17,96	19,09
RL-P37	Lactose	48	2	18,90	19,31	18,26	19,17	18,60	18,75	20,02

RL-P37	NaCl	6	1	18,65	18,72	17,40	19,12	17,35	19,03	19,31
RL-P37	NaCl	6	2	18,99	19,58	18,45	20,52	18,73	20,24	19,06
RL-P37	NaCl	24	1	20,41	20,26	19,01	20,44	19,86	20,59	20,88
RL-P37	NaCl	24	2	20,52	20,62	18,80	20,17	19,60	19,06	20,42
RL-P37	Xylan	48	1	21,61	21,61	19,76	21,06	21,12	19,03	20,49
RL-P37	Xylan	48	2	22,10	22,46	20,32	21,71	21,89	19,65	21,18
RL-P37	Xylan	24	1	18,51	19,46	19,45	20,80	20,26	19,86	21,67
RL-P37	Xylan	24	2	17,96	19,67	18,47	19,43	18,89	18,57	19,79
GEN-3A	Cellulose	120	1	21,18	21,19	19,97	20,89	20,37	20,45	21,61
GEN-3A	Cellulose	120	2	21,90	22,90	19,63	20,95	20,84	20,14	21,57
GEN-3A	Cellulose	48	1	19,48	18,22	18,95	20,04	19,09	19,21	20,36
GEN-3A	Cellulose	48	2	19,12	17,74	19,85	20,88	19,47	20,26	21,43
GEN-3A	DTT	6	1	19,19	25,27	19,92	21,34	19,95	20,42	21,53
GEN-3A	DTT	6	2	19,44	24,90	21,55	24,67	20,92	23,77	22,82
GEN-3A	DTT	48	1	21,70	27,03	18,42	19,22	19,41	18,27	19,26
GEN-3A	DTT	48	2	22,69	29,21	21,53	22,49	23,02	21,86	23,19
GEN-3A	Glucose	24	1	23,51	22,47	19,86	20,98	21,43	20,13	21,42
GEN-3A	Glucose	24	2	22,68	21,55	17,01	17,99	17,32	17,20	18,30
GEN-3A	Glucose	84	1	18,65	20,86	19,09	20,36	20,34	20,18	21,52
GEN-3A	Glucose	84	2	20,92	23,31	17,71	18,86	19,42	18,79	20,26
GEN-3A	Glycerin	24	1	20,07	21,12	17,99	19,28	19,49	18,58	20,05
GEN-3A	Glycerin	24	2	19,34	19,91	17,82	18,86	18,70	17,85	19,11
GEN-3A	Glycerin	84	1	18,67	19,24	17,81	18,87	18,02	18,08	19,14
GEN-3A	Glycerin	84	2	20,15	20,95	17,62	18,55	18,42	17,54	18,93
GEN-3A	Induced	96	1	25,56	25,49	22,14	22,83	23,98	21,81	23,04
GEN-3A	Induced	96	2	24,69	25,41	20,01	20,96	22,03	19,80	21,16
GEN-3A	Induced	48	1	23,37	23,33	21,62	22,32	22,80	21,50	22,58
GEN-3A	Induced	48	2	19,15	19,33	19,22	20,44	19,29	18,86	20,16
GEN-3A	Lactose	48	1	22,42	22,49	19,07	19,96	19,78	19,06	20,41
GEN-3A	Lactose	48	2	23,69	23,99	19,32	20,24	20,19	18,73	19,97
GEN-3A	Lactose	72	1	20,16	22,60	21,49	22,45	22,21	22,37	23,51
GEN-3A	Lactose	72	2	19,89	21,89	16,53	17,34	16,64	16,80	17,88
GEN-3A	NaCl	6	1	19,57	19,98	17,34	18,52	18,06	18,30	19,26
GEN-3A	NaCl	6	2	19,17	19,49	17,84	19,22	19,20	18,98	20,07
GEN-3A	NaCl	24	1	22,04	22,01	18,53	19,59	19,74	18,39	19,44
GEN-3A	NaCl	24	2	21,33	21,10	19,18	20,45	23,88	19,36	20,66
GEN-3A	Xylan	48	1	20,82	21,09	17,95	18,55	18,84	17,21	18,37
GEN-3A	Xylan	48	2	20,32	20,61	18,62	19,35	19,39	18,02	19,12
GEN-3A	Xylan	24	1	19,22	19,81	19,12	20,57	20,46	19,55	21,01
GEN-3A	Xylan	24	2	17,50	17,78	19,03	20,41	19,44	19,56	21,23

9.7 List of chemicals

Table 13: Chemicals used during the experiments

Chemical	Chemical formula	Manufacturer	Grade
Ammonium sulphate	$(NH_4)_2SO_4$	ROTH	≥ 99.5 %
Calcium chloride dihydrate	$CaCl_2 \cdot 2H_2O$	Merck	extra pure
Cellulose microcrystalline ca. 0.05 mm	$(C_6H_{10}O_5)_n$	SERVA	research grade
Citric acid monohydrate	$C_6H_8O_7 \cdot H_2O$	Merck	for analysis EMSURE® ACS, ISO, Reag. Ph Eur
Cobalt chloride hexahydrate	$CoCl_2 \cdot 6H_2O$	Merck	ACS,Reag. Ph Eur
di-Sodium hydrogen phosphate	$Na_2HPO_4 \cdot 2H_2O$	Merck	for analysis EMSURE®
Dithiothreitol (DTT)	$C_4H_{10}O_2S_2$	Thermo Fisher	98%
Ethanol 96 %	C_2H_6O	Merck	EMSURE® Reag. Ph Eur
Glucose monohydrate	$C_6H_{12}O_6 \cdot H_2O$	ROTH	≥99,5 %, Ph. Eur., USP
Glycerol	$C_3H_8O_3$	Merck	Ph Eur,BP,ChP,JP,USP,ACS
Iron sulphate heptahydrate	$FeSO_4 \cdot 7H_2O$	Merch	ACS,ISO,Reag. Ph Eur
Lactose monohydrate	$C_{12}H_{22}O_{11} \cdot H_2O$	Merck	for microbiology
Magnesium sulphate heptahydrate	$MgSO_4 \cdot 7H_2O$	ROTH	≥ 99 %
Manganese sulphate monohydrate	$MnSO_4 \cdot H_2O$	Sigma-Aldrich	ACS reagent, ≥98%
Peptone / tryptone from casein	-	ROTH	microbiology grade
Potassium dihydrogen phosphate	KH_2PO_4	ROTH	≥ 98 %
RNAzol® RT	-	Sigma-Aldrich	-
Sodium chloride	NaCl	Merck	Ph Eur,BP,JP,USP
Tween® 80	$C_{64}H_{124}O_{26}$	Merck	for synthesis
Urea	CH_4N_2O	Merck	GR for analysis ACS,Reag. Ph Eur
Xylan	$(C_5H_8O_4)_n$	ROTH	from beechwood
Zinc sulphate heptahydrate	$ZnSO_4 \cdot 7H_2O$	Merck	ACS reagent, ≥98%